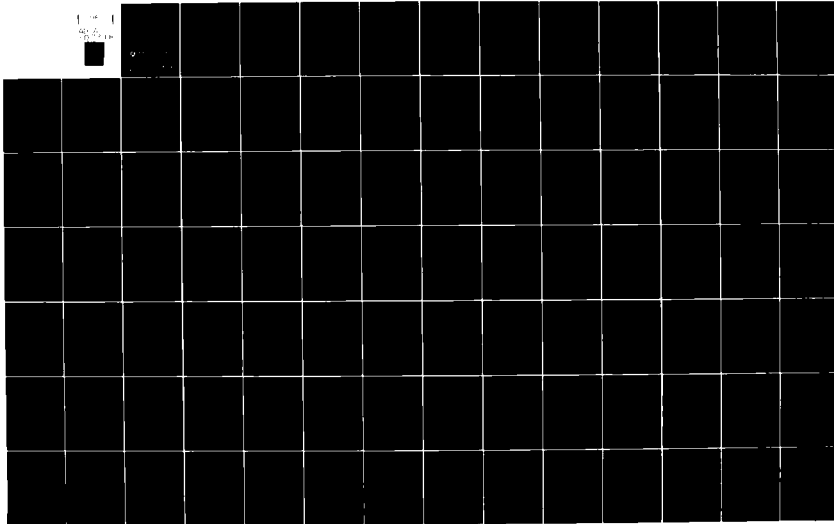


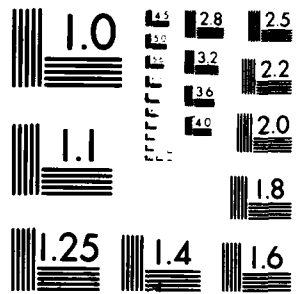
AD-A107 318

ARMY ARMAMENT RESEARCH AND DEVELOPMENT COMMAND ABERD--ETC F/O 80/4
A METHOD OF DETERMINING THE TURBULENT BASE PRESSURE IN UNIFORM --ETC(U)
OCT 81 T J MUELLER, L D KAYSER
ANBRL-TR-02374

UNCLASSIFIED

NL





MICROCOPY RESOLUTION TEST CHART
NATIONAL BUREAU OF STANDARDS-1963-A

LEVEL

12

AD

AD A107318

TECHNICAL REPORT ARBRL-TR-02374

A METHOD OF DETERMINING THE TURBULENT BASE
PRESSURE IN UNIFORM AND NON-UNIFORM
SUPERSONIC AXISYMMETRIC FLOWS

Thomas J. Mueller
Lyle D. Kayser

October 1981



US ARMY ARMAMENT RESEARCH AND DEVELOPMENT COMMAND
BALLISTIC RESEARCH LABORATORY
ABERDEEN PROVING GROUND, MARYLAND

Approved for public release; distribution unlimited.

DTIC
ELECTE
NOV 17 1981
S D D

FILE COPY

81 11 17 015

Destroy this report when it is no longer needed.
Do not return it to the originator.

Secondary distribution of this report by originating
or sponsoring activity is prohibited.

Additional copies of this report may be obtained
from the National Technical Information Service,
U.S. Department of Commerce, Springfield, Virginia
22151.

The findings in this report are not to be construed as
an official Department of the Army position, unless
so designated by other authorized documents.

*The use of trade names or manufacturers' names in this report
does not constitute endorsement of any commercial product.*

UNCLASSIFIED

SECURITY CLASSIFICATION OF THIS PAGE (When Data Entered)

REPORT DOCUMENTATION PAGE		READ INSTRUCTIONS BEFORE COMPLETING FORM
1. REPORT NUMBER TECHNICAL REPORT ARBRL-TR-82374	2. GOVT ACCESSION NO. AD-A107318	3. RECIPIENT'S CATALOG NUMBER
4. TITLE (and Subtitle) A METHOD OF DETERMINING THE TURBULENT BASE PRESSURE IN UNIFORM AND NON-UNIFORM SUPERSONIC AXISYMMETRIC FLOWS	5. TYPE OF REPORT & PERIOD COVERED Final rept.	
	6. PERFORMING ORG. REPORT NUMBER	
7. AUTHOR(s) Thomas J. Mueller Lyle D. Kayser	8. CONTRACT OR GRANT NUMBER(s)	
9. PERFORMING ORGANIZATION NAME AND ADDRESS U.S. Army Ballistic Research Laboratory (ATTN: DRDAR-BLL) Aberdeen Proving Ground, Maryland 21005	10. PROGRAM ELEMENT, PROJECT, TASK AREA & WORK UNIT NUMBERS RDT&E 1L162618AH80	
11. CONTROLLING OFFICE NAME AND ADDRESS U.S. Army Armament Research & Development Command U.S. Army Ballistic Research Laboratory (ATTN: DRDAR-BL) Aberdeen Proving Ground, MD 21005	12. REPORT DATE October 1981	
	13. NUMBER OF PAGES 95	
14. MONITORING AGENCY NAME & ADDRESS (if different from Controlling Office) 12 93	15. SECURITY CLASS. (of this report) Unclassified	
	15a. DECLASSIFICATION/DOWNGRADING SCHEDULE	
16. DISTRIBUTION STATEMENT (of this Report) Approved for public release, distribution unlimited.		
17. DISTRIBUTION STATEMENT (of the abstract entered in Block 20, if different from Report)		
18. SUPPLEMENTARY NOTES		
19. KEY WORDS (Continue on reverse side if necessary and identify by block number) Base Pressure Axisymmetric Flow Supersonic Flow		
20. ABSTRACT (Continue on reverse side if necessary and identify by block number) This report describes the base pressure computation procedure and computer program developed at the University of Notre Dame. The computation is valid for supersonic high Reynolds number flow at zero yaw. The computation is started upstream of the afterbody by means of the Method of Characteristics; hence, the effect of boattail, or flare, angle is determined. The effect of forebody shape can be indirectly determined if the external non-uniform Mach number profile is used as input for the start of the characteristics solution. However, the assumption of a uniform external flow generally provides good results. Examples		

UNCLASSIFIED

SECURITY CLASSIFICATION OF THIS PAGE(When Data Entered)

20. ABSTRACT (Continued).

are shown for uniform external flow inputs and for realistic non-uniform initial conditions. Also, results showing the effects of afterbody angle are presented.

Accession For	
NTIS GRA&I	<input checked="" type="checkbox"/>
DTIC TAB	<input type="checkbox"/>
Unannounced	<input type="checkbox"/>
Justification	
By	
Distribution/	
Availability Codes	
Dist	Avail and/or Special
A	

DTIC
ELECTE
NOV 17 1981
S D D

UNCLASSIFIED

SECURITY CLASSIFICATION OF THIS PAGE(When Data Entered)

TABLE OF CONTENTS

	<u>Page</u>
LIST OF ILLUSTRATIONS	5
INTRODUCTION	7
AXISYMMETRIC BASE PRESSURE PROBLEM	7
FORTRAN IV COMPUTER PROGRAM	12
COMPUTER PROGRAM DESCRIPTION	12
Method of Characteristics for Boattail and Flares	12
Base Pressure Solution	14
COMPUTER PROGRAM SUBROUTINES	17
DISCUSSION OF RESULTS FOR CONICAL AFTERBODIES	26
UNIFORM FLOW APPROACHING THE AFTERBODY	26
NON-UNIFORM FLOW APPROACHING THE AFTERBODY	27
CONCLUSION AND RECOMMENDATIONS	28
FIGURES	29
REFERENCES	48
LIST OF SYMBOLS	49
APPENDIX A - SYMBOL DEFINITION	53
APPENDIX B - OPERATING INSTRUCTIONS	71
APPENDIX C - BOATTAIL/FLARE-BASES COMPUTER PROGRAM INPUT AND OUTPUT FOR THE ABERDEEN PROVING GROUND UNIVAC 1108 (SAMPLE CASES INCLUDED)	79
APPENDIX D - COMPUTER PROGRAM FLOW CHARTS	87
DISTRIBUTION LIST	93

BLANK PAGE

LIST OF ILLUSTRATIONS

Figure	Page
1. Geometric Configurations of Interest	29
a. Cylindrical Body	
b. Conical Boattail Afterbody	
c. Conical Flare Afterbody	
d. Cone	
2. Flow Model for the Influence of Initial Flow Direction on the Axisymmetric Turbulent Base Pressure	30
3. Trailing Wake Radius Ratio Versus Mach Number for $\gamma = 1.4$ (Ref. 6)	31
4. Schematic of Axisymmetric Characteristic Grid	32
5a. Characteristic Construction Technique (I - odd number) .	33
5b. Characteristic Construction Technique (I - even number).	33
6. Characteristic Numbering Scheme	34
7. Characteristic Termination Lines	35
8. Variation of X_2 , R_2 , v_2 , θ_2 along a Characteristic Line, 2	36
9. Sketch of the Afterbody Configurations for the Method of Characteristics Solution	37
a. Boattailed Body of Revolution	
b. Flared Body of Revolution	
10. Interpolation Scheme Used in Subroutine LINEAR	38
11. Variation of Separation Pressure Ratio with Mach Number from Zukowski (Ref. 9)	39
12a. Characteristics Mesh Before Reaching XFIN	40
12b. Characteristics Mesh After Reaching XFIN	40
12c. Corrected Characteristics Mesh Done by Subroutine SETUP.	40
13a. Qualitative Behavior of Function Subprogram FSTEP4	41
13b. Searching Scheme Used to Locate the Regions of Solution in SOTE2B	41
13c. Interval Halving Technique Used in SOTE2B	41

LIST OF ILLUSTRATIONS (CONT.)

Figure		Page
14.	The Influence of Boattail Angle on the Base Pressure Ratio for a Uniform Initial Flow	42
15.	Base Pressure Ratio Versus Mach Number for Uniform Flow Approaching Boattail	43
16.	Influence of Conical Afterbody Angle on the Base Pressure Ratio for a Fixed Afterbody Length	44
17.	Influence of Initial Mach Number on Base Pressure Ratio for a Fixed Afterbody Length	45
18.	Base Pressure Ratio Versus Boattail Angle for Uniform and Non-Uniform Flow	46
19.	Comparison of the Calculated Base Pressure Ratio for Uniform Flow with BRL Data	47

INTRODUCTION

The analytical determination of the pressure acting on the blunt base of axisymmetric supersonic vehicles has been under consideration for more than two decades. Although a successful analytical approach for the plane two-dimensional turbulent supersonic base pressure problem with uniform external flow approaching the base evolved in the early 1950's, an equally successful and straightforward analytical method for the axisymmetric case was not developed until the late 1960's. In a review of base drag research by Sedney¹ in 1966, it was concluded that no satisfactory theory existed. The principal objectives of the work described herein were to modify and improve the method of calculating the turbulent base pressure in axisymmetric supersonic flow, develop a computer program using this method, and compare computed results with those from experiments for cases of interest to the U.S. Army Ballistic Research Laboratory, ARRADCOM.

AXISYMMETRIC BASE PRESSURE PROBLEM

Analytical studies were conducted to evaluate the utility, for the present task, of the mathematical base pressure model for axisymmetric supersonic flow as developed by Zumwalt² and modified by Mueller, et al^{3,4}. It was found that this turbulent flow model offered the best possibility of predicting the base pressure for high Reynolds number flows and for including the effects of base bleed and Reynolds number later with a minimum of computer time. The configurations of interest in this investigation are shown in Figure 1. For high Reynolds numbers, the turbulent boundary layers on the short bodies shown in Figure 1 are usually very thin, while the inviscid flow upstream of the base in 1a and 1d or upstream of the afterbody in 1b and 1c may be uniform or non-uniform.

1. Sedney, R., "Review of Base Drag", BRL Report No 1337, U.S. Army Ballistic Research Laboratory, Aberdeen Proving Ground, Maryland, October 1966. AD 808767
2. Zumwalt, G. W., "Analytical and Experimental Study of the Axially-symmetric Supersonic Base Pressure Problem, Ph.D. Dissertation", University of Illinois, 1959.
3. Mueller, T. J., "Determination of the Turbulent Base Pressure in Supersonic Axisymmetric Flow". *Journal of Spacecraft and Rockets*, Vol. 5, No. 1, pp. 101-107, January 1968.
4. Mueller, T. J., and Hall, C. R., Jr., "Analytical Prediction of the Turbulent Base Pressure in Supersonic Axisymmetric Flow Including the Effect of Initial Flow Direction". AFFDL-TR-68-132, September 1968.

The computer program, called BOATTAIL/FLARE-BASE 5, uses the axisymmetric method of characteristics to calculate the flow over conical boattailed and flared bodies of revolution. This calculation yields the necessary initial flow field for the base pressure determination. This program can be used to calculate the turbulent base pressure for configurations similar to all those in Figure 1. Both non-uniform and uniform supersonic flows approaching the base or afterbody can be handled.

The theoretical flow model used in conjunction with the axisymmetric method of characteristics for the flow over boattails and flares is shown in Figure 2. In this model, the flow is divided into three components: (a) an inviscid free stream, (b) a dissipative mixing layer and (c) a base region. In addition to using the restricted mixing theory of Korst⁵, the following conditions are imposed on these three flow components:

- (i) The boundary layer approaching the separation corner is neglected although it is assumed to be fully turbulent.
- (ii) An isentropic expansion takes place in the free stream from 1 to 2, i.e., a continuation of the axisymmetric method of characteristics for the flow over the afterbody.
- (iii) The inviscid flow past a conetail using axisymmetric characteristics is utilized to define the pressure field impressed on the mixing region from 2 to 3. The conetail surface also serves as the "corresponding inviscid jet boundary".
- (iv) The pressure normal to the "corresponding inviscid jet boundary" is assumed to be constant within and near the mixing region at each cross-section.
- (v) Velocity profile similarity is assumed in the mixing region. The error function velocity distribution is located within the intrinsic system of coordinates x, y . The coordinate shift between the reference coordinates X, Y and the intrinsic coordinates x, y is represented by $X = x$ and $Y = y - y_m(x)$ where $y_m(0) = 0$. This coordinate shift is a result of using the restricted mixing theory of Korst.

5. Korst, H.H., "A Theory for Base Pressures in Transonic and Supersonic Flow". *Journal of Applied Mechanics*, Vol. 23, No. 4, pp. 593-600, December 1956.

- (vi) The axisymmetric geometry of the mixing region is taken into account in the integral presentation for momentum and mass flux between sections 2 and 3.
- (vii) Recompression is assumed to result from an oblique shock turn from 3 to 4 at the empirically determined trailing wake radius. Values for the flow over cylindrical bodies are given by Chapman⁶, and are reproduced in Figure 3.

A streamline, j , can be identified which divides the amount of mass passing over the corner at 1 from that mass flow entrained by the viscous action of the free jet mixing region. A second streamline, d , can be identified which has just sufficient kinetic energy at 3 to negotiate the pressure rise to 4. Streamlines below the d -streamline have lower kinetic energies and are unable to pass through recompression and are turned back to recirculate in the base region. If there is no secondary flow, i.e., no mass bleed into or out of the base region, the conservation of mass requires that the j - and d -streamlines be identical. Korst distinguished between these two streamlines and pictured the space between them as a sort of corridor through which mass would flow into or out of the base region.

The control volume utilized in the formulation of the conservation of mass and momentum between cross-sections 2 and 3 is bounded by streamlines R and $-R$ as shown in Figure 2. The streamlines R and $-R$ were defined by Zumwalt² so that the cross-sectional area normal to the direction of flow would remain nearly constant and the $P dA$ pressure force could be neglected in the momentum equation. This condition is retained in the present development although its validity is questionable. For the simplified axisymmetric flow model described above, Zumwalt formulated the momentum equation in the axial direction using geometrical relations and the relation between the inviscid and viscid coordinate systems. This equation was solved simultaneously with the combined viscid and inviscid continuity equations written for the control volume between cross-sections 2 and 3. For the error function velocity profile, $\phi = 1/2(1 + \text{erf } \eta)$ where $\phi = u/u_a$ and $\eta = \sigma y/x$, it was found that $\eta R = 3$ was large enough for ϕ_j to approach its asymptotic value. The result of this analysis is a nonlinear equation which allows one to locate the j -streamline at cross-section 3, namely:

6. Chapman, D.R., "An Analysis of Base Pressure at Supersonic Velocities and Comparison with Experiment". NACA Report 1051, 1951. (Supercedes NACA TN-2137, 1950.)

$$\{(B - 3)^2 + 2(1 - C_{3a}^2)[I_1]_{-\infty}^{\eta} - I_1[\eta]_{-\infty}^{\eta}\} B - 2(1 - C_{3a}^2)[J_1]_{-\infty}^{\eta} - J_1[\eta]_{-\infty}^{\eta} = \left(\frac{\sigma r}{r \cos \theta}\right)_{3a}^2 \quad (1)$$

where the integral limits refer to η values, and

$$B = \frac{J_1[\eta]_{-\infty}^{\eta} - [1 - (C_{3a}/C_{2a})]J_1[\eta]_{-\infty}^{\eta} - (C_{3a}/C_{2a})(J_1 - J_2)[\eta]_{-\infty}^{\eta}}{I_1[\eta]_{-\infty}^{\eta} - [1 - (C_{3a}/C_{2a})]I_1[\eta]_{-\infty}^{\eta} - (C_{3a}/C_{2a})(I_1 - I_2)[\eta]_{-\infty}^{\eta} + [(\gamma - 1)/\gamma](3 C_{2a}C_{3a})[1 - (P_2/P_3)]} \quad (2)$$

$$I_1 = \int_{-\infty}^{\eta} \frac{\phi d\eta}{1 - C_{3a}^2 \phi^2} \quad (3)$$

$$I_2 = \int_{-\infty}^{\eta} \frac{\phi^2 d\eta}{1 - C_{3a}^2 \phi^2} \quad (4)$$

$$J_1 = \int_{-\infty}^{\eta} \frac{\phi \eta d\eta}{1 - C_{3a}^2 \phi^2} \quad (5)$$

$$J_2 = \int_{-\infty}^{\eta} \frac{\phi^2 \eta d\eta}{1 - C_{3a}^2 \phi^2} \quad (6)$$

It is important to notice that, since these integrals are expressed only in terms of Crocco number, they are independent of γ although Equation 1 is a function of γ .

It is evident that, to determine ϕ_{j3} from Equations 1 and 2 for a given initial condition, the location of the recompression region, \bar{r}_3/r_b , the corresponding inviscid condition, M_{3a} and the jet spread parameter, σ_{3a} , must be known. The location of the recompression region, \bar{r}_3/r_b , is determined from the experimental data for cylindrical bodies and is replotted in Figure 3. Unfortunately, the effect of initial flow direction on the wake radius ratio does not appear to have been documented experimentally or, if it has, it has not been

published in the open literature. The Mach number along the inviscid jet boundary from 2 to 3, i.e., M_{3a} , is determined from the axisymmetric characteristics solution. The jet spread parameter, σ_{3a} , is determined from the equation obtained by Channapragada⁶:

$$\sigma_{3a} = \{R[1 + \beta(1 - C_{3a}^2)]\}^{-1} \sigma_{inc} \quad (7)$$

where $\sigma_{inc} = 12$ for the error function velocity profile used, $\beta = T_{oa}/T_b = 1$ for isoenergetic mixing considered here, and R is the empirical compressible divergence factor defined by Channapragada⁷ and presented as a function of Crocco number.

The geometric parameter, $[\sigma \bar{r}/x \cos\theta]_{3a}^2$, may be calculated, since $\theta_{3-4} = \theta_{1-2}$ from the conical wake assumption and since

$$\left[\frac{\sigma \bar{r}}{x \cos\theta} \right]_{3a}^2 = \left[\frac{\sigma \tan\theta}{[1/(\bar{r}/r_b)] - 1} \right]_{3a}^2 \quad (8)$$

At this point $\phi_{j3} = \phi_{d3}$ (i.e., no base bleed) may be obtained from Equations 1 and 2; therefore, $C_{d3} = \phi_{d3} C_{3a} = \phi_{j3} C_{3a}$ is calculated for isoenergetic flow. However, the value of C_{d3} can also be obtained from the assumed isentropic recompression mechanism along the d-streamline (i.e., $P_{o3d} = P_4$), from

$$C_{d3} = \{1 - (P_4/P_3)^{-[(\gamma - 1)/\gamma]}\}^{1/2} \quad (9)$$

where P_4/P_3 is the pressure rise across the two-dimensional oblique shock which results from the turning of the flow with Mach number M_{3a} through the angle θ_{3-4} . When the two values of C_{d3} are equal, then the assumed base pressure ratio is the correct one for the given conditions at 1.

The flow model used for constant pressure jet mixing is identical to the flow model used in the previous section, except that assumption (iii) of the previous section is discarded and replaced by the

7. Channapragada, R.S., "Compressible Jet Spread Parameter for Mixing Zone Analyses". *AIAA Journal*, Vol. 1, No. 9, pp. 2188-2189, September 1963.

assumption that the velocity of the jet adjacent to (but outside of) the mixing region is constant in magnitude although not in direction. For this situation, $\theta_{1-2} \neq \theta_{3-4}$ and the shape of the "corresponding inviscid jet boundary" is determined from the axisymmetric method of characteristics as a constant pressure jet boundary. The value of ϕ_{j3} is obtained from Equations 1 and 2 by setting $P_b = P_2 = P_3$ and $C_{3a} = C_{2a}$.

FORTRAN IV COMPUTER PROGRAM

A FORTRAN IV computer program for the UNIVAC 1108 digital computer was developed to calculate the axisymmetric flow field over conical boattailed and flared bodies of revolution using the axisymmetric method of characteristics. The results of this calculation provide the necessary initial flow field for the base pressure determination which forms the second part of the total computer program. Complete program symbols, usage and listing are presented in Appendices A, B and C.

COMPUTER PROGRAM DESCRIPTION

Because of the complex and unique nature of this program, a serious effort directed toward understanding its operation and limitations is recommended before it is run on the computer.

Method of Characteristics for Boattails and Flares

A schematic of an axisymmetric characteristic grid is shown in Figure 4. Values of the variables X, R, v , and θ are determined at the $I=1$ position, and the calculation of the remainder of the points is obtained from these initial conditions and the boundary conditions along the walls. The calculation procedure sweeps diagonally as shown by the arrow in Figure 4. The calculations begin at a point off the surface of the body revolution, and proceed outward until the limit of the matrix is reached at the $I=1$ location. The limit referred to here is the limit on J since I is a constant ($= 1$) at this location. For the interior flow field points (i.e., those points not on the surface of the body), the subroutine KBPR.CALC is called which determines the values of the variables at a new grid point further downstream. From Figure 5a it is noted that for I an odd number, the position of the point $(I+1, J)$ may be determined from the left running wave of the $(I, J-1)$ point and the right running wave of the (I, J) grid point. Once the X and R coordinates of this new $(I+1, J)$ grid point have been established, the additional variables of v and θ may be determined. For I being an even number, the (I, J) and $(I, J-1)$ grid points are used to determine the $(I+1, J-1)$ grid point (see Figure 5b).

The key to the mesh system of the characteristic solution is that there are no $J=1$ points when I is an even number (see Figure 6). It should be noted that the first number in the parenthesis will be the value of the subscript I , while the second number refers to the subscript J . In doubly-subscripted variables, I is along the axis of the body, while J is in the radial direction. For singly-subscripted variables, the subscript I is not confined to any particular location, but instead refers to the order of points.

On the body surface and on the conetail surface in the base pressure solution, the location of a characteristic grid point is obtained by use of the subroutine KBPR.SURF. Since the $J=1$ point always falls on the surface itself, only the $(I-1,2)$ point is required to locate the new $(I,1)$ point. This is because the value of θ at the surface is known (i.e., θ at the surface is parallel to the surface). The characteristic solution continues until a point on the surface exceeds the end point of the body (or the end point of the portion of the body being considered), XFIN. From this point, the subroutine KBPR.SETUP is called in an effort to locate a grid point on the body as close to this end point as possible. Actually, KBPR.SETUP is called twice to further refine the initial correction. Once the characteristic line to this point has been established, the characteristics solution proceeds to line ① or line ② as shown in Figure 4. Location ① (or ②) is read into the program depending on the type of output desired. Location ① refers to a constant I output (not necessarily a straight line), while location ② is the output along a characteristic line. Again, it should be emphasized, that even though the last point on the surface, XFIN, has been determined, the characteristics solution still proceeds until the values of J have been exhausted at the $I=1$ position. The characteristics solution then proceeds only to this line ① (or ②), thus eliminating needless calculations.

Once the characteristics solution has been completed for the section of the body of revolution being considered, the values of the variables X, R, v and θ along ① (or ②) are tabulated separately. To avoid confusion, these variables are now referred to as $X2, R2, v2$ and $\theta2$ (see Figure 7). When XFIN is greater than the starting value of $X(1,1)$, there are always fewer values of the variables at any location in the characteristics matrix than there are at the $I=1$ location. This is because of the inherent nature of the characteristics solution at a free boundary (see Figure 4). The tabulated values of $X2, R2, v2$ and $\theta2$ are now stored and may be used to further proceed with another characteristics solution for another downstream section of the body of revolution. It should be noted that these variables need only one subscript since the line ① (or ②) describes the location in space. The subscript merely refers to the order of the points, i.e., $I=1$ refers to the point on the body, $I=2$ is the next point out, etc.

An independent variable is now introduced, and the values of X_2 , R_2 , v_2 and θ_2 are assumed to be functions only of this new variable, D . More precisely, D measures the distance from the body surface along the line ① (or ②). This independent variable, D , is defined as:

$$D(I) = D(I-1) + \sqrt{[X_2(I) - X_2(I-1)]^2 + [R_2(I) - R_2(I-1)]^2}$$

This equation shows that $D(I)$ is the linear distance of some grid point from the preceding grid point plus the sum of the linear distances from previous grid points. Thus the following relations of X_2 , R_2 , v_2 and θ_2 vs. D are shown qualitatively in Figure 8 for the case of the output being along a characteristic (line ②). Therefore, for any distance along ② (or ①) there are values of X_2 , R_2 , v_2 and θ_2 available.

The characteristics solution now proceeds to the next section of the body of revolution. Before the solution continues, however, a full starting matrix of X, R, v and θ must be determined at the new $I=1$ position. This is obtained by defining a new independent variable, $D_1(I)$. Both $D_1(I)$ and $D(I)$ are distances measured along ① (or ②). However, $D_1(I)$ defines the grid spacing required to re-start the characteristics solution for the new region. These new grid spacings are functions of the boattail (or flare) angle, and also the surface Mach number. Once these values of D_1 have been determined, values of X, R, v and θ are obtained along ① (or ②) by interpolating the values of X_2, R_2, v_2 and θ_2 of Figure 8. The KBPR.TAB sub-program which allows any order interpolation up to order 10 is used to carry out this operation. The characteristics solution is now set to proceed through this new region of the body. The calculation procedure is identical to that described above, and only minor changes in computer logic are made with each section (except the base pressure solution).

This above discussion of the characteristics solution refers primarily to the subroutine KBPR.FLARE which directs the actual calculation of the characteristics solution along the body of revolution. Flow Chart 1 in Appendix D indicates the operation of KBPR.FLARE.

Base Pressure Solution

The calculation procedure in the base pressure section of the computer program may be divided into seven major steps. The following description of the calculation procedure is taken essentially from reference 2. The flow model is shown in Figure 2.

- Step 1: A base pressure ratio P_b/P_1 (= PBPI) is assumed and the corresponding value of the inviscid jet boundary angle (THET12), and M_{2A} are obtained from a Prandtl-Meyer expansion from region 1 to 2. The Crocco number, C_{2A} , is obtained from the relation:

$$C_{2A}^2 = \frac{M_{2A}^2}{\frac{2}{\gamma-1} + M_{2A}^2} \quad (10)$$

Step 2: The value of the wake radius ratio, R_w/R_b (= RSRB), is obtained from the function subprogram KBPR.RSBF. The Mach number ratio M_{3a}/M_{2a} (= M3AM2A) is obtained from an axisymmetric method of characteristics solution of the near wake flow field. Then the Crocco numbers, C3A and C3A/C2A, are determined as functions of M3A and M2A; also the angle of the inviscid jet boundary, THET3A, is obtained.

Step 3: The jet spread parameter at the recompression, S3A, is calculated (in the subprogram KBPR.SIGMA) as a function of M3A. The geometric parameter, GP, is then calculated using:

$$GP = \left[\frac{S3A \times \tan(\text{THET12})}{(1/\text{RSRB}) - 1} \right]^2 \quad (11)$$

Step 4: The velocity ratio PHIJ3 is now solved from a complicated functional relationship:

$$\text{PHIJ3} = \phi_{j3} = \text{fcn}(GP, M3A, G, C3A/C2A)$$

Specifically, ϕ_{j3} is found from:

$$\phi_{j3} = \frac{1}{2} (1 + \text{erf } \eta_{j3}) \quad (12)$$

where η_{j3} is the value of the upper integral limit which satisfied:

$$\text{KBPR.FSTEP4} = \{(B-3)^2 + 2(1-C^2)[BI_1 \Big|_{\eta_j}^{\infty} - J_1 \Big|_{\eta_j}^{\infty}]\} - GP = 0 \quad (13)$$

where B is given by Equation 2, and the integrals I_1 , I_2 , J_1 and J_2 are given by Equations 3, 4, 5 and 6, respectively. The error function may be expressed:

$$\text{erf}(\eta) = \frac{2}{\sqrt{\pi}} \int_0^{\eta} e^{-\alpha^2} d\alpha \quad (14)$$

and erf (η) is evaluated in the function subprogram KBPR.ERF.

The pressure ratio, P_2/P_3 , is determined from isentropic relations, and from the Mach number ratio, M_{2A}/M_{3A} , obtained in Step 2.

Step 5: For steady flow with no mass bleed, C_{d3} (=C5) may be determined from:

$$C_{d3} \equiv C_5 = \phi_{j3} C_{3A} \quad (15)$$

Step 6: The pressure ratio, P_4/P_3 , is then calculated from the oblique shock relations with the initial Mach number being M_{3A} and the turning angle being THET_{3A} . With isentropic recompression assumed along the dividing streamline, then:

$$C_{d3} \equiv C_6 = \left[1 - \frac{1}{\left(\frac{P_4/P_3}{\frac{\gamma-1}{\gamma}} \right)^{\frac{1}{2}}} \right] \quad (16)$$

Step 7: The subroutine KBPR.BASE5 takes the difference between $C_{d3} \equiv C_5$ (obtained in Step 5) and $C_{d3} \equiv C_6$ (obtained in Step 6). When $C_5 \approx C_6$, a solution is obtained. New estimates of the base pressure are made by using the subroutine KBPR.LINEAR until $C_5 \approx C_6$, indicating a solution has been reached. The basic convergence scheme for this base pressure analysis is shown schematically in Flow Chart 3 in Appendix D. A general Flow Chart of the base pressure section of the report is shown in Flow Chart 4 in Appendix D.

There are two possible solutions which may be used in the base pressure analysis. Both involve axisymmetric method of characteristics solutions. These options are:

- a) Conetail solution (IBOUND=1) in which $\text{THET}_{12} = \text{THET}_{3A}$. However, $M_{3A} \neq M_{2A}$.
- b) Constant pressure boundary solution (IBOUND=2) in which $M_{3A} = M_{2A}$. In this case, however, $\text{THET}_{12} \neq \text{THET}_{3A}$.

In some cases, the stability of the program depends on the initial estimate of the base pressure, PEST, which is read into the program. In general, a flared body requires

a more accurate guess than a boattailed afterbody. If the range of a solution is not known, it is better to estimate a low base pressure ratio for flared bodies. For boattailed afterbodies, much more latitude is permissible in estimating the base pressure ratio. However, for large boattail angles ($> 12^\circ$), a high estimate of PEST should be used.

High Mach numbers also present some problems. In general if the Mach number is high (> 4.0), a more accurate PEST is required. Also, to increase the stability of the scheme at high Mach numbers, IOUT should be read in as 1.

Low Mach numbers over flared bodies also may present difficulties. In general, the Mach number at the tip of the base should not be less than 1.30. In addition, special care should be taken such that the Mach number along the flare does not become subsonic.

COMPUTER PROGRAM SUBROUTINES

A complete list of the subroutines and a brief description of their operation are given below.

KBPR.CNTR0L

KBPR.CNTR0L is the main program in the calculation procedure (see Flow Chart 2 in Appendix D). Its function is to direct the other programs in the correct sequence. Data for this operation of the characteristics solution are read in by this program. In addition, the various options associated with the characteristics solution are determined here. The relative simplicity of this program makes it possible to perform supplementary calculations and include additional steps without changing the more complex subprograms. In particular, this program directs the calculation of the flow field over the body. The direction of the base pressure solution is controlled by the subroutine KBPR.BASE5 which is called by KBPR.CNTR0L.

KBPR.FLARE

The subroutine KBPR.FLARE directs the actual calculation of the characteristics solution both over the body (see Figure 9) and in the near wake region. KBPR.FLARE sets up the grid spacing of the initial characteristic. It also calculates various Mach numbers and angles associated with the base pressure solution.

KBPR.LCHAR

The subroutine KBPR.LCHAR determines the line 1 (or 2) as shown in Figures 4 and 8. This subroutine is also responsible for stopping characteristic calculations beyond this line so that useless computations are not made. The variables X2, R2, v2 and θ2 are the results obtained from this subroutine.

KBPR.SIMR

KBPR.SIMR is a function subprogram which performs a Simpson's Rule integration of a function between the limits of X1 and XN. The integration is divided into N equal intervals where N must be an even number. This subprogram was developed by Professor R.S. Eikenberry of the University of Notre Dame Aero-Space Department.

KBPR.DINCR

The subroutine KBPR.DINCR performs the geometric calculations which determines how large physically, the characteristics solution has to be such that there are sufficient points to complete the calculations. This returns the increment of spacing between grid points for the three locations: along the body, along the flare or boattail, and in the near wake region. These spacings are functions of the initial Mach number, the flare (or boattail) angle, and the body length.

KBPR.A11

The function KBPR.A11 is the argument of the I1 integral used in the base pressure solution, i.e.:

$$KBPR.A11 = \frac{\phi dn}{1 - C_{3a}^2 \phi^2}$$

KBPR.A12

KBPR.A12 is a function subprogram which defines the argument of the I2 integral used in the base pressure solution, i.e.:

$$KBPR.A12 = \frac{\phi^2 dn}{1 - C_{3a}^2 \phi^2}$$

KBPR.AJ1

The function KBPR.AJ1 defines the argument of the J1 integral used in the base pressure solution, i.e.:

$$\text{KBPR.AJ1} = \frac{\phi \eta \, d\eta}{1 - C_{3a}^2 \phi^2}$$

KBPR.AJ2

The function KBPR.AJ2 defines the argument of the integral J2 which is used in the base pressure solution, i.e.:

$$\text{KBPR.AJ2} = \frac{\eta^2 \eta \, d\eta}{1 - C_{3a}^2 \phi^2}$$

KBPR.I1

The function KBPR.I1 evaluates the I1 integral between specific limits using a Simpson's Rule integration (KBPR.SIMR).

KBPR.I2

KBPR.I2 is a function subprogram which evaluates the I2 integral using Simpson's Rule integration.

KBPR.J1

KBPR.J1 is a function subprogram which evaluates the J1 integral using Simpson's Rule integration.

KBPR.J2

The function KBPR.J2 evaluates the J2 integral using Simpson's Rule integration.

KBPR.BODY

The subroutine KBPR.BODY calculates the distance XBASE (i.e., the axial location of the base). It should be noted that this calculation is also done in KBPR.CNTR0L, and for the present, KBPR.BODY is limited to a diagnostic program; it tells if body shapes other than conical flares or boattails are used. This subprogram is still included since, in the future, additional afterbody configurations may be studied which would necessitate such a subroutine.

KBPR.TAB

This function subprogram evaluates a single function for a given argument by interpolation between tabulated values. The maximum table size is 16,384 entries, and the maximum degree of interpolation is ten. Table search is by a binary method requiring 15 steps to find any entry in a table of 16,384 entries. Interpolation (for order of interpolation greater than 1) is done by means of Lagrange Polynomials. If the argument is outside the limits of the table, the first (or last) tabular entry is returned to the calling program. This subprogram was developed by Prof. R.S. Eikenberry of the Aero-Space Department at the University of Notre Dame.

KBPR.ERF

The function subprogram KBPR.ERF evaluates the error function for a given argument.

KBPR.PRES

The subroutine KBPR.PRES calculates the Mach number, pressure coefficient (C_p), and the pressure ratio (P/P_o) at the different X-locations on the surface of the body. (It should be noted that the characteristics solution assumes an inviscid fluid and, therefore, the no-slip condition on the body surface is not applicable.) The Mach number is obtained by the use of the subroutine KBPR.PMTURN. The pressure ratio, P/P_o , is determined from:

$$P/P_o = \left[1 + \frac{\gamma-1}{2} M^2 \right]^{\frac{-\gamma}{\gamma-1}}$$

The pressure coefficient (based on the free stream Mach number) is expressed in the form:

$$C_p = \frac{P/P_\infty - 1}{\frac{1}{2} \gamma M_\infty^2}$$

The values of X, M, P/P_o and C_p are printed out at each location in KBPR.CNTROL.

KBPR.RSBF

This function subprogram⁸ is used to calculate the effective sting radius ratio which is used in the base pressure solution. For the present, there is no dependence on the ratio of specific heats, γ , only the Mach number at the tip of the base. In the near wake, the characteristics solution proceeds until a grid point is encountered which is less than this sting radius (wake radius). In KBPR.FBASE5, a linear interpolation of the variables is made to this sting radius.

KBPR.SIGMA

This function subprogram⁸ calculates the jet spread parameter, σ . The jet spread parameter used in the base pressure analysis is that formulated by Channapragada⁷. The incompressible value of the jet spread parameter, σ_{inc} , has been assumed to be 12.0.

KBPR.LINEAR

The subroutine KBPR.LINEAR solves by successive linear interpolations the value of XS which satisfies $FCN(XS) = 0 \pm ACX$ where ACX is an accuracy requirement. In the base pressure program, $FCN = KBPR.FBASE5 = C5 - C6$ and XS is the solution for P_b/P_1 . XEST is the initial estimate of the base pressure ratio (PEST), and DXLIN is the size of the first interval of the independent variable (see Figure 10).

The values of YEST = FCN(XEST) and Y1 = FCN(XEST-DXLIN) are calculated. The slope, $S(= \frac{Y1 - YEST}{DXLIN})$, is used to project toward a new estimate of the solution, X2. Then Y2 = FCN(X2) is evaluated. If $Y2 = 0 \pm ACX$, then X2 is taken as the solution and a return is made to the calling program. If not, the slope is then taken between Y2 and Y1 and this new slope is projected again toward the value of the independent variable, X3. This process is repeated until convergence is reached by satisfying the accuracy requirement.

KBPR.CALC

The subroutine KBPR.CALC is used to solve for the characteristics solution of points which are in the interior flow field (i.e., not boundary points). The procedure for calculating the location of a new

8. Roache, P.J., and Mueller, T.J., "A FORTRAN IV Program for Calculating the Axisymmetric Base Pressure in Turbulent Supersonic Flow (BASE1)". UNDAS TN-866-M1, University of Notre Dame, Aerospace Engineering, August 1966.

grid point is an iterative one for the axisymmetric method of characteristics since the equation is no longer homogeneous. Actually, two iterations are used and this yields satisfactory results for a reasonable grid spacing. Once the X and R coordinates of this grid point have been determined, the value of the streamline angle, θ , and the Prandtl-Meyer turn angle, ν , are calculated for that point.

The two upstream points which are used to calculate this new point are determined by the subroutine KBPR.FLARE which calls for KBPR.CALC.

KBPR.SURF

KBPR.SURF is the subroutine which calculates the variables X, R, ν and θ on the surface of the body (or on the conetail surface in the base pressure analysis). Again this becomes an iterative procedure, and two guesses are made. As the geometry is known, it is only necessary to match up X and R with θ , as θ at the surface is the angle of the surface. Once this has been done, the value of ν on the surface is calculated. Again this subroutine is directed by the subroutine KBPR.FLARE.

KBPR.CPB

This subroutine provides a constant pressure boundary base pressure solution. Again this is an iteration procedure, and two iterations are made. In a constant pressure boundary solution, the value of ν remains unchanged. Therefore, the correct combination of X, R and θ satisfy this criterion. This subroutine is directed again by KBPR.FLARE.

It should be noted that this subroutine is not called for a constant pressure boundary solution until the flow has passed through the Prandtl-Meyer expansion at the base. To calculate the characteristics through this expansion, the subroutine KBPR.SURF is called by KBPR.FLARE.

KBPR.SEP RTE

This subroutine called by KBPR.CNTROL determines if there is flow separation on the surface of a boattailed afterbody. The separation criterion which is used compares pressure ratios at the surface with a separation pressure ratio for that free stream Mach number given by Zukowski⁹ and shown in Figure 11. If the pressure ratio indicates separation, a message is printed which relates the pressure ratio which was encountered and also the axial distance of separation. It should be noted that the separation criterion used is valid only for free stream Mach numbers between 1.50 and 6.50. For Mach numbers not within this range, the separation criterion is not applied.

9. Zukowski, E.E., "Turbulent Boundary Layer Separation in Front of a Forward-Facing Step". *AIAA Journal*, Vol. 5, No. 10, pp. 1746-1753, October 1967.

KBPR.SETUP

The KBPR.SETUP subroutine is used in an attempt to locate a grid point on the surface of the body which is as close to the end of the body (or region of the body) as possible. Referring to Figure 12a, it is noted that the characteristics solution on the surface has not yet exceeded the end point, XFIN. However, in Figure 12b, the succeeding characteristic solution on the surface has exceeded XFIN. A linear interpolation is now made between X(I-2,1) and X(I,1) such that:

$$RTO = \frac{X(I,1) - XFIN}{X(I,1) - X(I-2,1)}$$

where RTO is the ratio of these two distances. It should be noted that on the surface, only odd values of I appear (see Figure 6) and, therefore, X(I-2,1) is used instead of X(I-1,1). The value of D1 which resulted in the point is "lowered" proportionally to RTO. That last characteristic line is recalculated. The results of this procedure are shown in Figure 12c. The whole procedure is again repeated to achieve further accuracy. The KBPR.SETUP subroutine then makes normal return to the subroutine KBPR.FLARE and the remainder of the characteristic lines are calculated.

KBPR.PMTURN

This subroutine solves the inverse Prandtl-Meyer turn equation of an ideal-gas compressible flow. It either returns the downstream Mach number after an isentropic turn, or simply determines the Mach number for a given Prandtl-Meyer turn angle, ν , where ν is defined as:

$$\nu = \sqrt{\frac{\gamma + 1}{\gamma - 1}} \tan^{-1} \sqrt{\frac{\gamma - 1}{\gamma + 1} (M^2 - 1)} - \tan^{-1} \sqrt{M^2 - 1}$$

Calculations are made using a Newton-Raphson technique.

KBPR.PMANGL

KBPR.PMANGL is a function subprogram which solves the Prandtl-Meyer turn equation of an ideal-gas, compressible flow. It returns the Prandtl-Meyer turn angle, ν , which is defined by the Equation above.

KBPR.SOTE2B

The subroutine KBPR.SOTE2B solves a double-valued transcendental equation $FCN(XS) = 0 \pm AC$, where AC is an accuracy requirement. In the base pressure analysis, FCN is the function FSTEP4(ETAJ3). This is a complicated integral equation to be solved for $\eta_{j3} = \text{ETAJ3}$, the upper limit of integrals I2 and J2. To use SOTE2B, the upper extreme, XU, and the lower extreme, XL, must be defined. The values of XU and XL have been set at +3 and -3, respectively. The indicator, IND = +1, causes the upper solution to be given, while IND < 0 gives the lower solution.

Figure 13a shows the qualitative behavior of FSTEP4 and illustrates the method of solution. The range of X for a solution is first reduced to a ΔX which contains the upper solution XS (for IND = +1), but not the lower solution. To do this a search is initiated for a sign change in FSTEP4 as X is decreased from XU = +3. To avoid possibly skipping over the sign changes, the technique shown in Figure 13b is used. The sweeps continue until a sign change is found between some X1 and X2. Now the problem is reduced to finding a solution XS to a single-valued transcendental equation in which XS is known to lie between X1 and X2. The solution is found by interval halving which is shown in Figure 13c. The calculation proceeds A-B-C-D-E in which the interval is decreased by half at each trial. This technique is very rapid as n-calculations reduce the interval size to less than $(1/2)^n$ of its initial size.

KBPR.SHOCK

The subroutine KBPR.SHOCK gives a closed-form solution of the shock wave cubic equation for an ideal gas. It returns to the calling program the wave angle when the initial Mach number and streamline turn angle are given. If the detachment turn angle is exceeded, the value returned is the detachment turn angle. The indicator, N=4, provides a weak shock solution, while N=0 gives the strong shock solution. The form of the exact solutions may be found in Reference 7. This program was developed by Patrick J. Roache of the Aero-Space Department at the University of Notre Dame.

KBPR.FSTEP4

The function subprogram KEPR.FSTEP4 is the subprogram in the base pressure section of the program which combines the integrals resulting in the calculation of the geometric parameter. The difference between the actual geometric parameter and the calculated geometric parameter is what is transferred into KBPR.SOTE2B.

KBPR.BASE5

The subroutine KBPR.BASE5 is the program which directs the calculation of the base pressure at the rear of the body. This subroutine is called by KBPR.CNTROL after the flow field over the body has been established. In KBPR.BASE5, the parameters for the operation of the base pressure section of the program are read in. This subroutine is primarily used for reading data and printing out the variables once a solution has been obtained.

KBPR.FBASE5

This function subprogram is called by KBPR.BASE5 and is the directing program in the base pressure analysis. The effective sting radius (see KBPR.RSBF) is determined and then the geometric parameter

is obtained. The subroutine KBPR.FLARE is used to direct the axisymmetric method of characteristics in the near wake region. KBPR.FBASE5 calls KBPR.SOTE2B in which convergence on a base pressure ratio is achieved.

DISCUSSION OF RESULTS FOR CONICAL AFTERBODIES

A large amount of experimental afterbody and base pressure data have been taken for boattailed bodies of revolution. These investigations include conical, circular arc and parabolic shaped boattails of various length to diameter ratios for Mach numbers from about 1.7 to about 6.0. Because of the possible occurrence of flow separation as well as model support or sting interference, these data must be examined very carefully before comparisons can be made with the analytical results.

The computer program BOATTAIL/FLARE-BASE5 can be used to calculate the turbulent base pressure for configurations similar to all those shown in Figure 1. Both non-uniform and uniform flows approaching the base or afterbody can be handled. Sample inputs with the corresponding outputs are included in Appendix C.

UNIFORM FLOW APPROACHING THE AFTERBODY

This computer program has been used and the results verified for uniform approach Mach numbers from 1.3 to 5.0, ratios of specific heats from 1.2 to 1.667, base temperature ratios from 0.5 to 3.0, and conical boattail and flare angles up to 15°. A few examples of the type of results obtained from this program will be presented. All analytical results in this report are for the case of rising pressure jet mixing.

The results obtained from the BOATTAIL/FLARE-BASE5 computer program for $\gamma = 1.4$, $T_b/T_{oa} = 1.0$ and an initial uniform Mach number of 2.0 are shown in Figure 14. The geometry of the boattail body studied analytically was the same as that studied experimentally by Reid and Hastings¹⁰ so that a direct comparison could be made. The experiments of Reid and Hastings closely approximate the analytical flow model used i.e., uniform external flow except for a relatively thin turbulent boundary layer. Other data available either include nose effects, angle of attack of effects and/or an undetermined boundary layer character and thickness approaching the base. Excellent agreement between the present analytical method and the data of Reid and Hastings is indicated in Figure 14 for $r_b/r_c = 0.58$. The computer solution was unable to

10. Reid, J., and Hastings, R.C., "Experiments on the Axi-Symmetric Flow Over Afterbodies and Bases at $M = 2.0$ ". Royal Aircraft Establishment Report No. Aero.2628, October 1959, (STAR N66-20065).

produce reliable results for boattail angles ($-\phi$) lower than about 3° because of the grid spacing of the characteristics solution necessary to achieve accuracy. For small angles and moderate r_b/r_c , the boattail (or flare) length becomes quite long, requiring a large grid size. However, if the curve of Figure 14 is extrapolated to a boattail angle of zero, the resulting base pressure ratio agrees with the results for the flow over a cylindrical body obtained by Mueller³, i.e., $P_b/P_1 \doteq 0.6$. Results for a 7° boattail and $\gamma = 1.4$, $T_b/T_{oa} = 1.0$, $L/r_c = 0.75$ for Mach numbers from 1.3 to 5.0 are shown in Figure 15.

The influence of afterbody angle, ϕ , on the base pressure ratio for initial uniform Mach numbers 2.0, 3.0 and 4.0 is presented in Figure 16. These results were obtained for a fixed afterbody length, $L/r_c = 0.5$, a uniform initial Mach number, $\gamma = 1.4$, and $T_b/T_{oa} = 1.0$. Figure 17 shows the influence of initial Mach number on the base pressure ratio for several afterbody angles and a longer afterbody. In this figure a fixed afterbody length of $L/r_c = 2.0$, i.e., a one caliber afterbody, was used with a uniform initial Mach number, $\gamma = 1.4$, and $T_b/T_{oa} = 1.0$. These results indicate the well behaved nature of the analytical results for conical afterbodies. If desired, this method could be used to study the influence of afterbody shape, γ , and T_b/T_{oa} on the base pressure ratio. A sample input and output from BOATTAIL/FLARE-BASE5 for uniform flow of $M = 3.0$ approaching a one caliber 7° boattail is shown at the end of Appendix C.

NON-UNIFORM FLOW APPROACHING THE AFTERBODY

A large amount of effort has been expended to study the use of BOATTAIL/FLARE-BASE5 for non-uniform supersonic flows approaching the afterbody. For one of these studies a linear Mach number distribution approaching a conical boattail with $L/r_c = 0.5$ was chosen. The non-uniform Mach number profile was input at the end of the cylindrical body and ranged from $M_c = 2.10$ at the body surface, i.e., $r/r_c = 1.0$, to $M_\infty = 2.3$ at $r/r_c = 1.6$ from the body surface. The freestream at $M_\infty = 2.3$ was continued to $r/r_c = 2.0$. The conical boattail angle was varied from 0° to 9° . A comparison of the base pressure ratio calculated for a uniform flow with $M_c = 2.3$ and the linear non-uniform flow is presented in Figure 18 as a function of boattail angle. This non-uniform Mach number profile produces base pressure ratios which are lower than the values obtained for uniform flow.

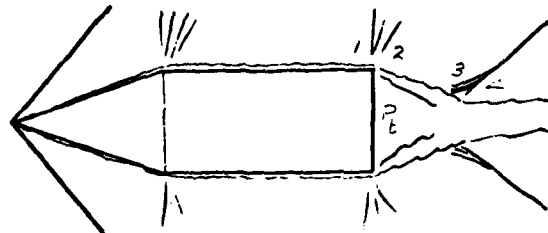
To compare the base pressure ratios calculated using BOATTAIL/FLARE-BASE5 with experimental values for a particular U.S. Army configuration, several specific cases were run. The configuration studied had a three caliber secant ogive nose, a two caliber cylindrical section and a one caliber 7° conical boattail. The non-uniform Mach number distribution just upstream of the boattail, obtained from a BRL solution of the Euler Equations using MacCormack's predictor-corrector numerical technique¹¹. This non-uniform input, along with the corresponding output, is shown at the end of Appendix C. Figure 19 presents a comparison of the computed results for this non-uniform flow input as well as for many uniform flow cases with the BRL experimental data. As the non-uniform Mach number distribution was close to a uniform profile, it is not surprising that this result falls on the uniform flow curve. The fact that the experimental data for the highest Reynolds number tested also fall on this curve is an indication of how well base pressure ratio is predicted by BOATTAIL/FLARE-BASE5.

It was found by L.D. Kayser of BRL that this program could also be used to obtain base pressure results for cones. By choosing a fairly long flare with an angle equal to the cone angle and a uniform Mach number, results which agreed well with experimental data were obtained.

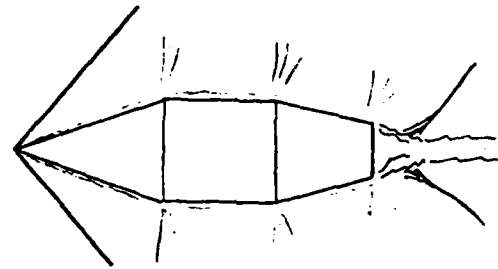
CONCLUSION AND RECOMMENDATIONS

The computer program now operational on the Aberdeen Proving Ground UNIVAC 1108 has been found to produce results which agree well with experimental data for high Reynolds numbers. These programs will run for a wide variety of geometries and approach flow conditions and can even be used to calculate base pressure on cones. These programs can be modified, if desired, to include the effects of base bleed and initial boundary layer thickness.

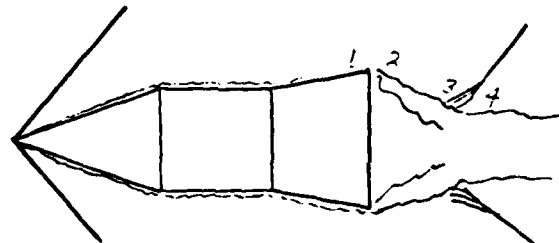
11. Sanders, B.R., "Three-Dimensional, Steady Inviscid Flow Field Calculations with Application to the Magnus Problem", PhD Dissertation, University of California, Davis, California, May 1974.



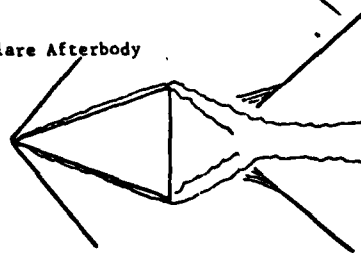
a.) Cylindrical body



b.) Conical Boattail Afterbody



c.) Conical Flare Afterbody



d.) Cone

Figure 1. Geometric Configurations of Interest

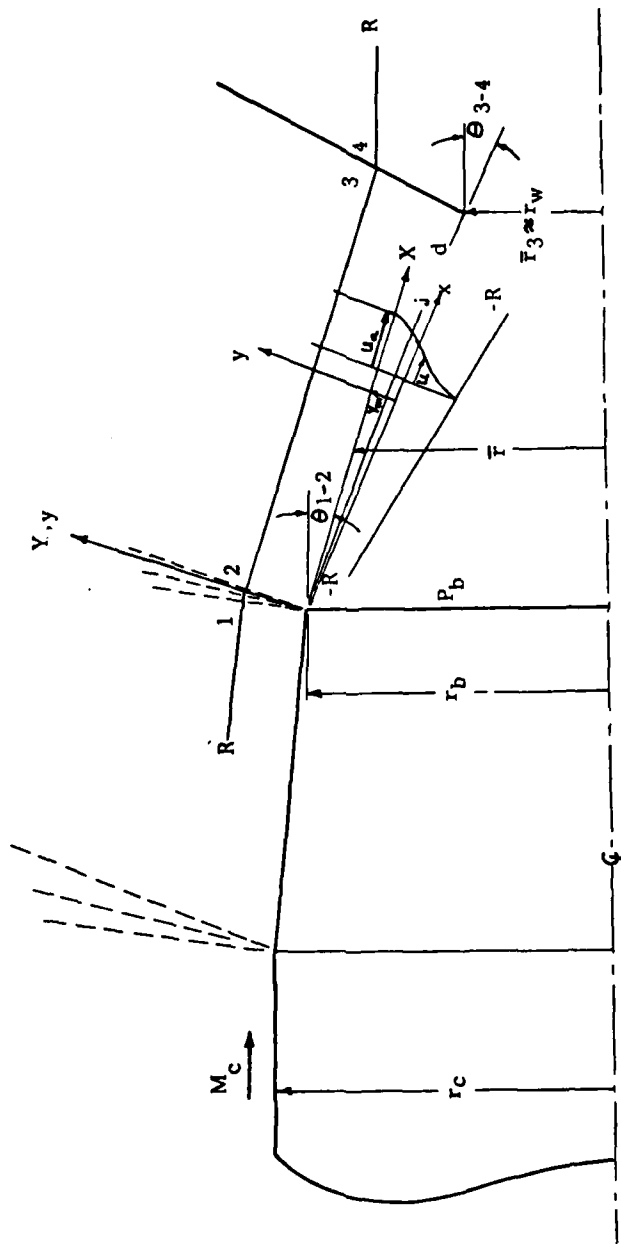


Figure 2. Flow Model for the Influence of Initial Flow Direction on the Axisymmetric Turbulent Base Pressure.

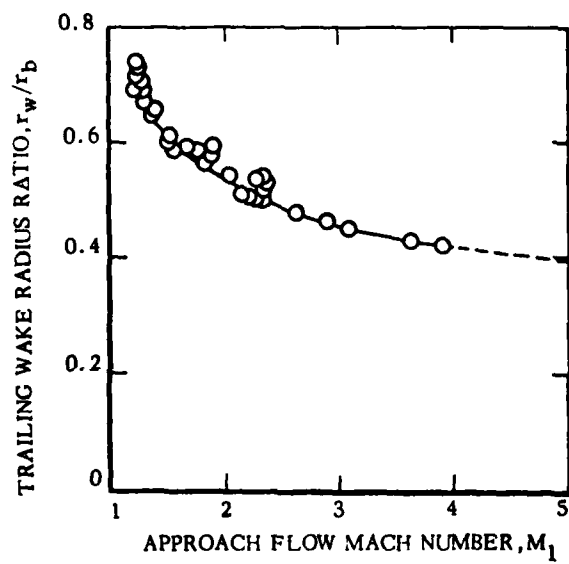


Figure 3. Trailing Wake Radius Ratio Versus Mach Number for $\gamma = 1.4$ (Ref. 6)

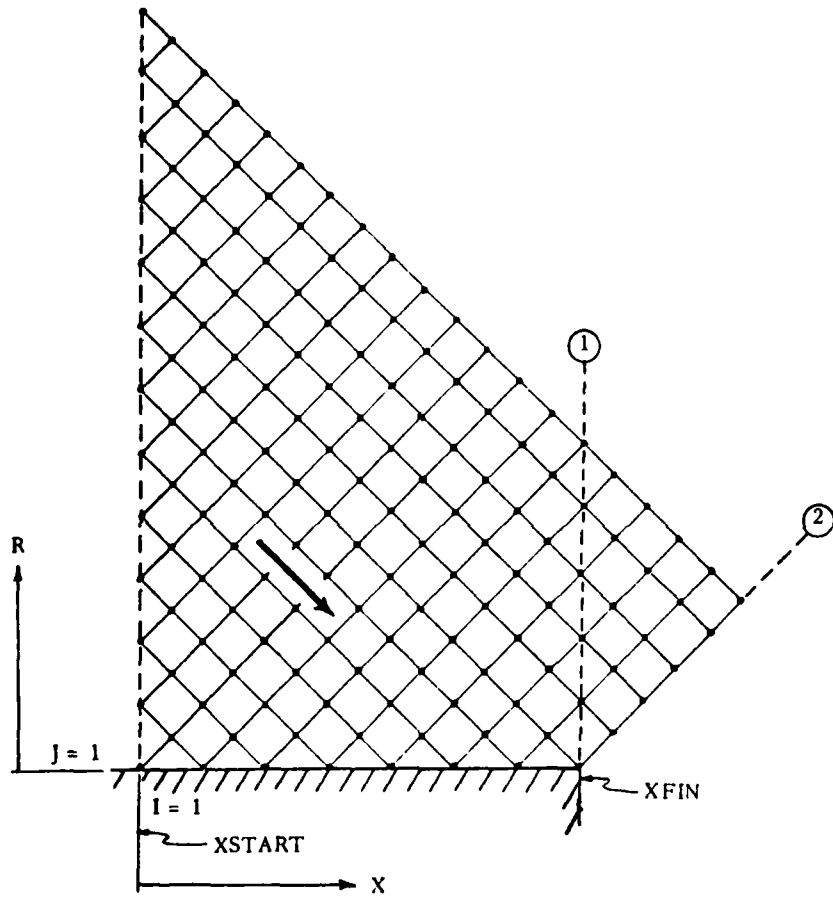


Figure 4. Schematic of Axisymmetric Characteristic Grid

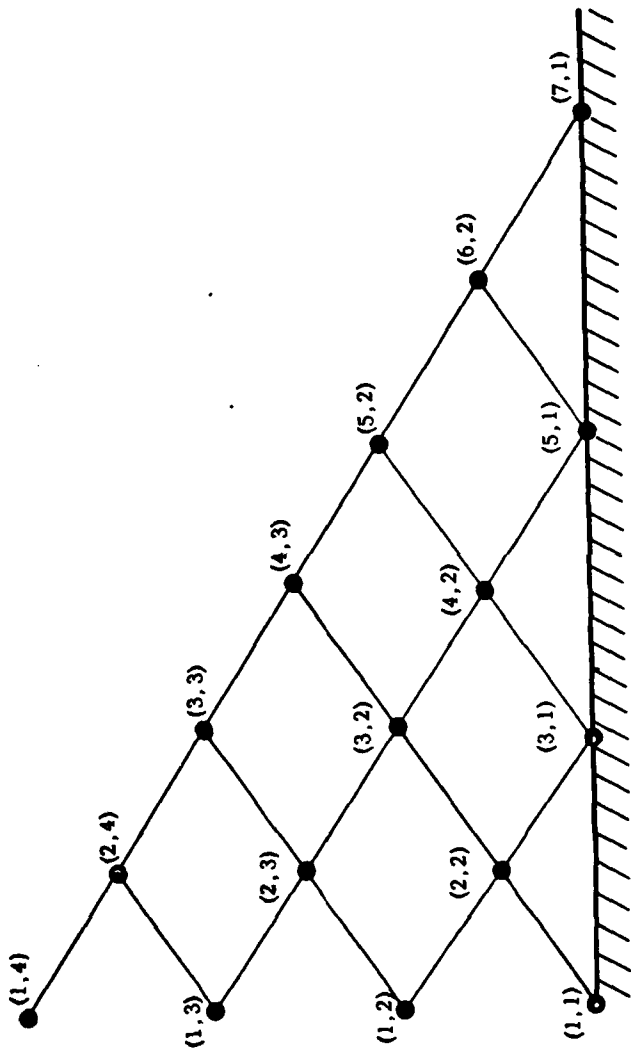


Figure 6. Characteristic Numbering Scheme

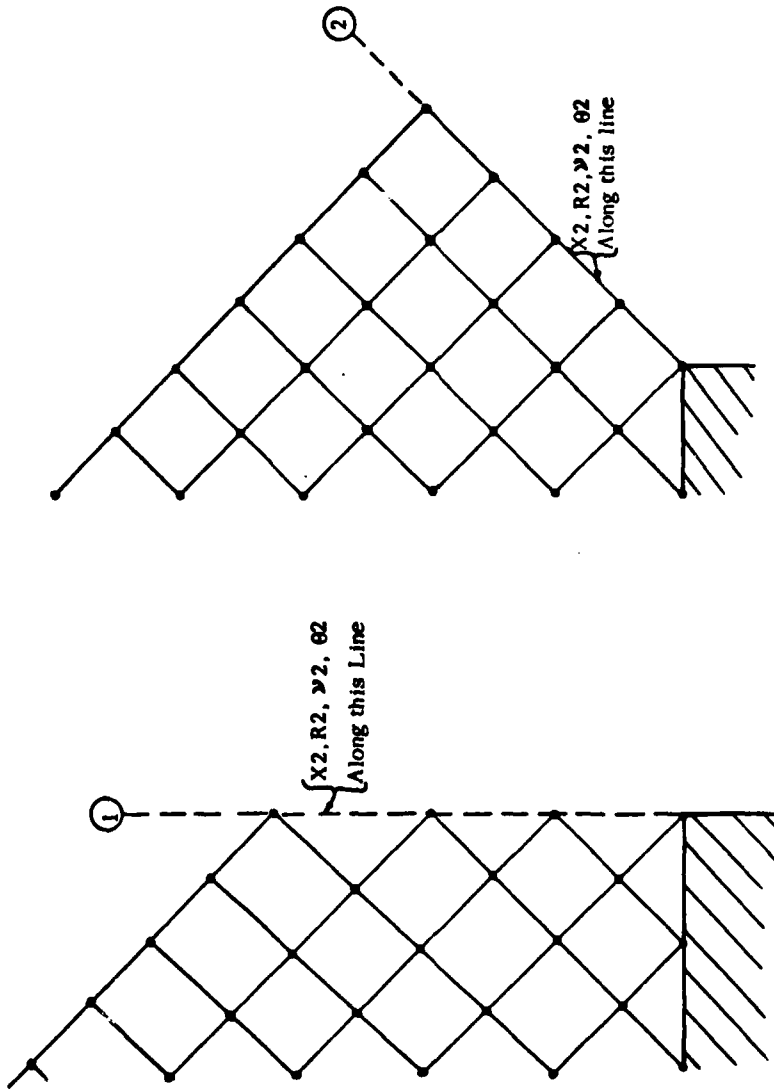


Figure 7. Characteristic Termination Lines

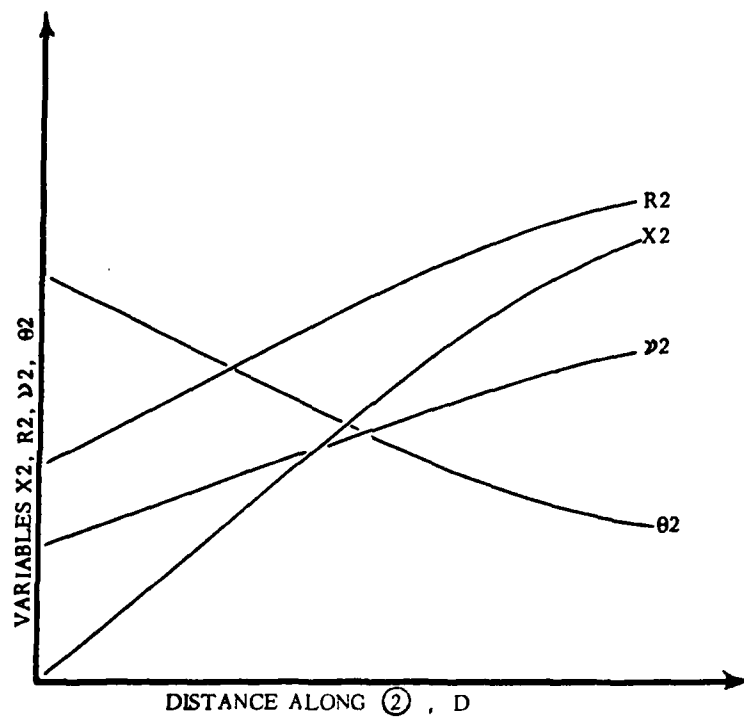
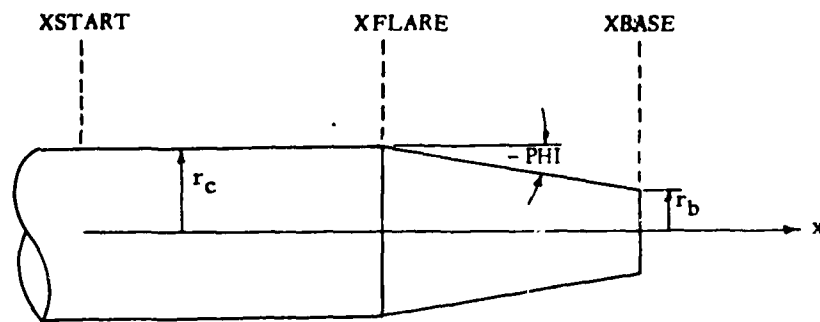
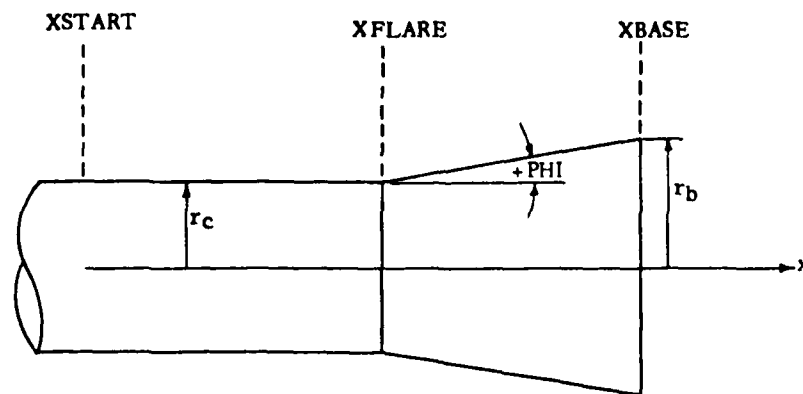


Figure 8. Variation of X_2 , R_2 , v_2 , θ_2 along a Characteristic Line, 2



a. Boattailed Body of Revolution



b. Flared Body of Revolution

Figure 9. Sketch of the Afterbody Configurations for the Method of Characteristics Solution.

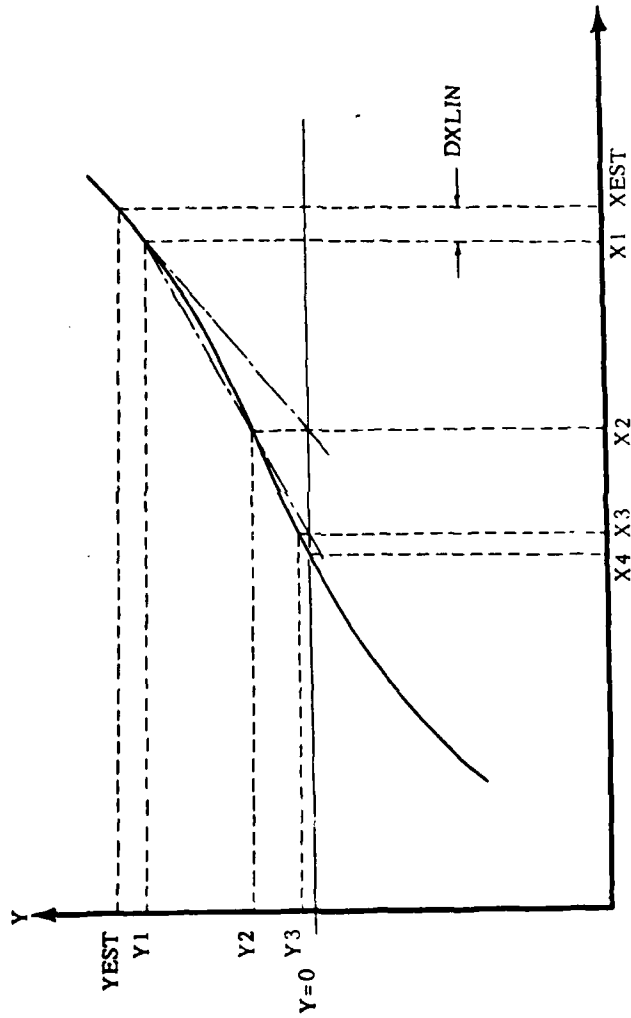


Figure 10. Interpolation Scheme Used in Subroutine LINEAR

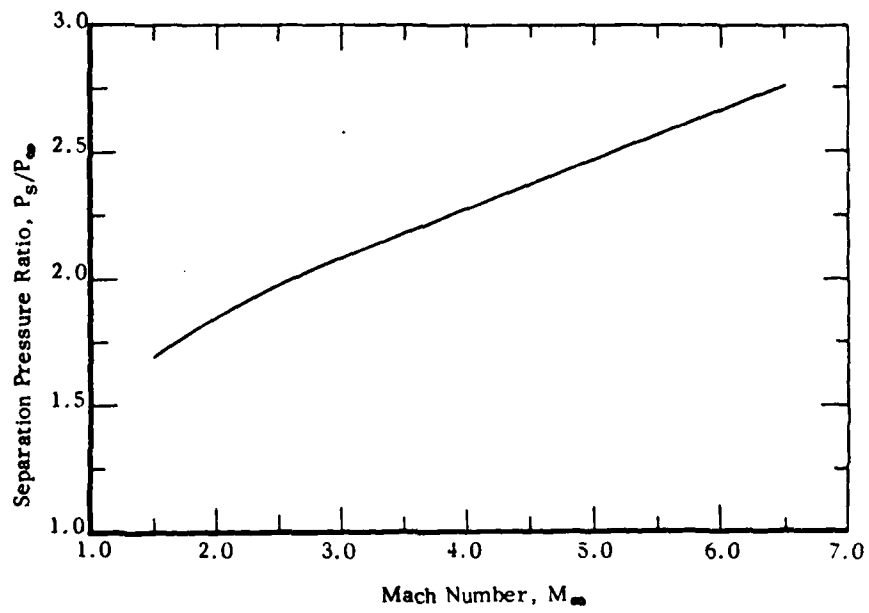


Figure 11. Variation of Separation Pressure Ratio with Mach Number from Zukowski (Ref. 9)

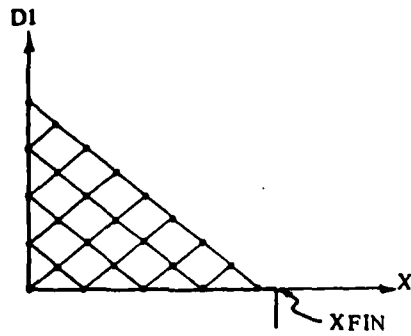


Figure 12a. Characteristics Mesh Before Reaching XFIN

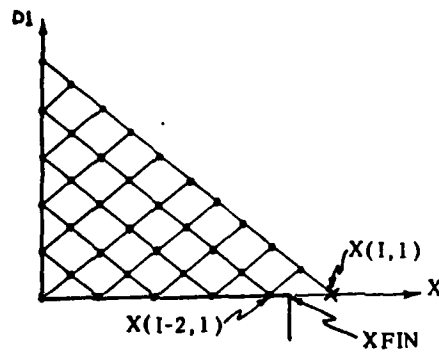


Figure 12b. Characteristics Mesh After Reaching XFIN

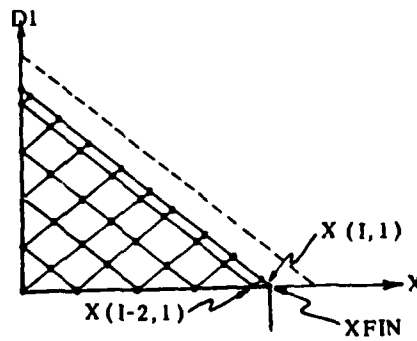


Figure 12c. Corrected Characteristics Mesh Done by Subroutine SETUP

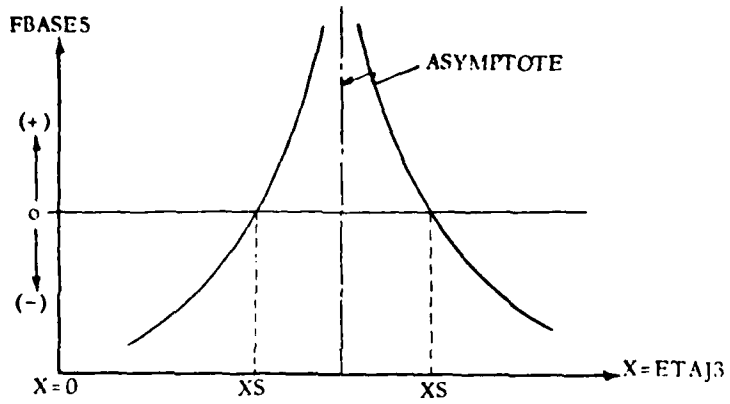


Figure 13a. Qualitative Behavior of Function Subprogram FSTEP4

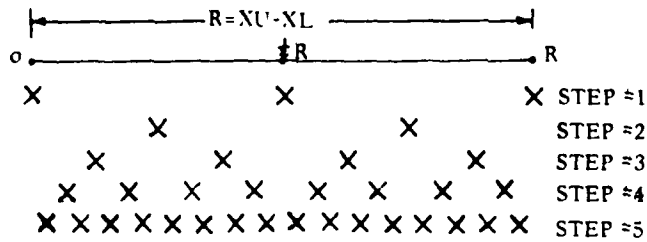


Figure 13b. Searching Scheme Used to Locate the Regions of Solution in SOTE2B

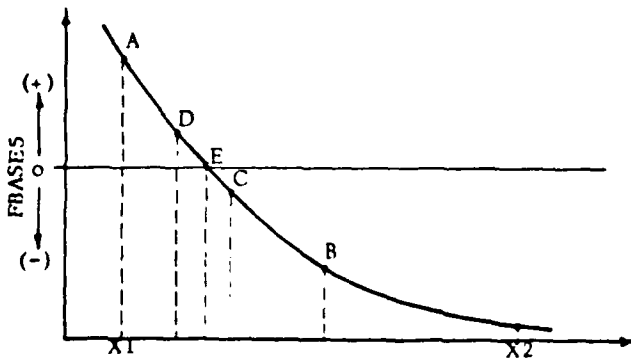


Figure 13c. Interval Halving Technique Used in SOTE2B

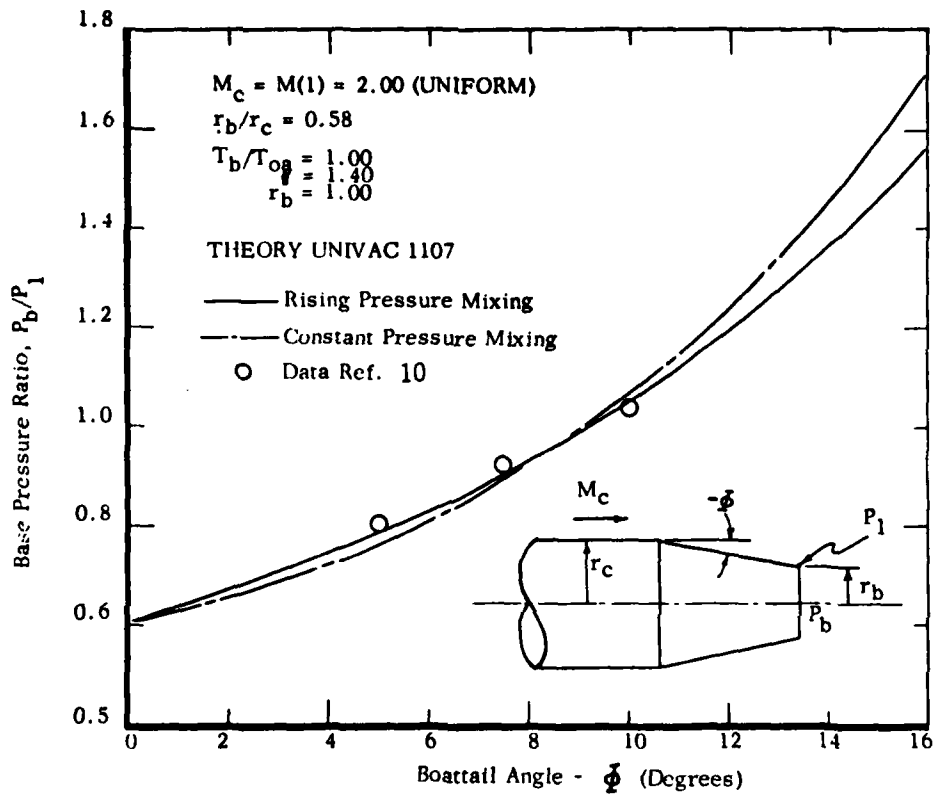


Figure 14. The Influence of Boattail Angle on the Base Pressure Ratio for a Uniform Initial Flow

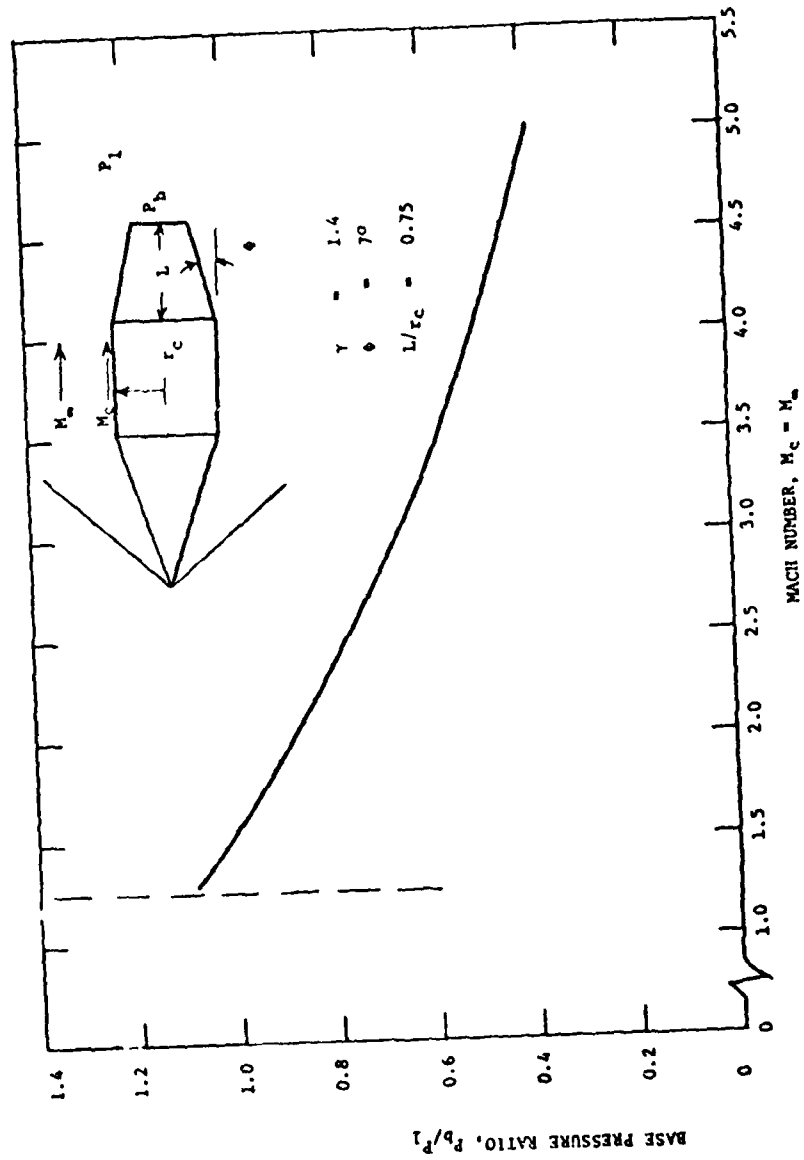


Figure 15. Base Pressure Ratio Versus Mach Number for Uniform Flow Approaching Boattail

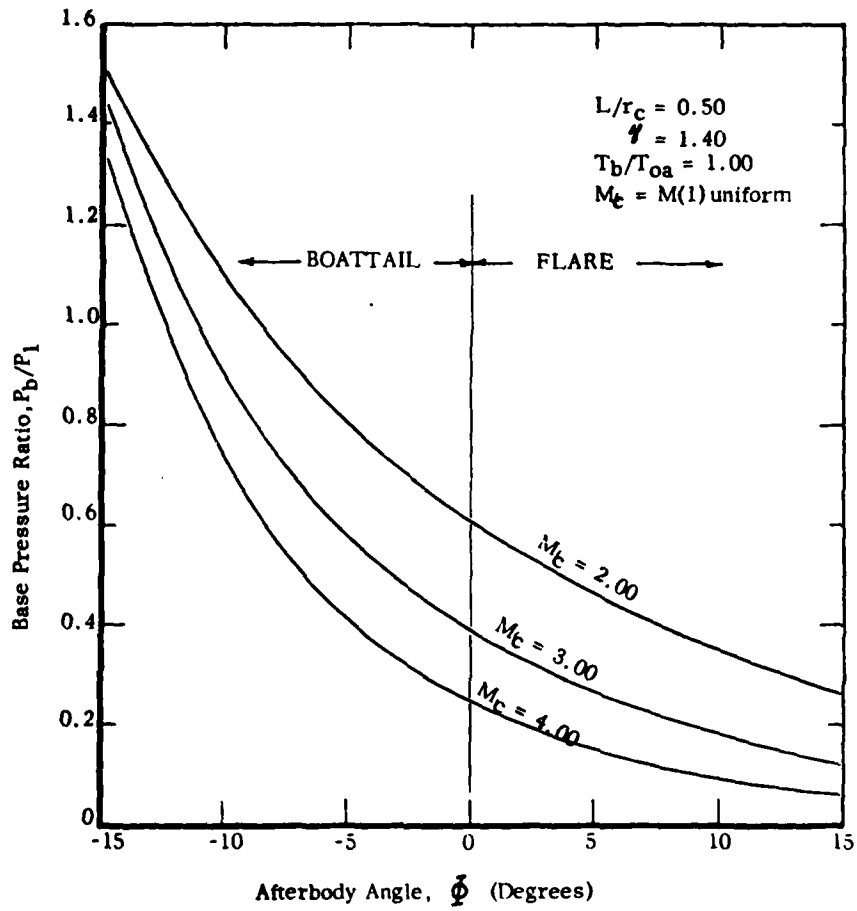


Figure 16. Influence of Conical Afterbody Angle on the Base Pressure Ratio for a Fixed Afterbody Length

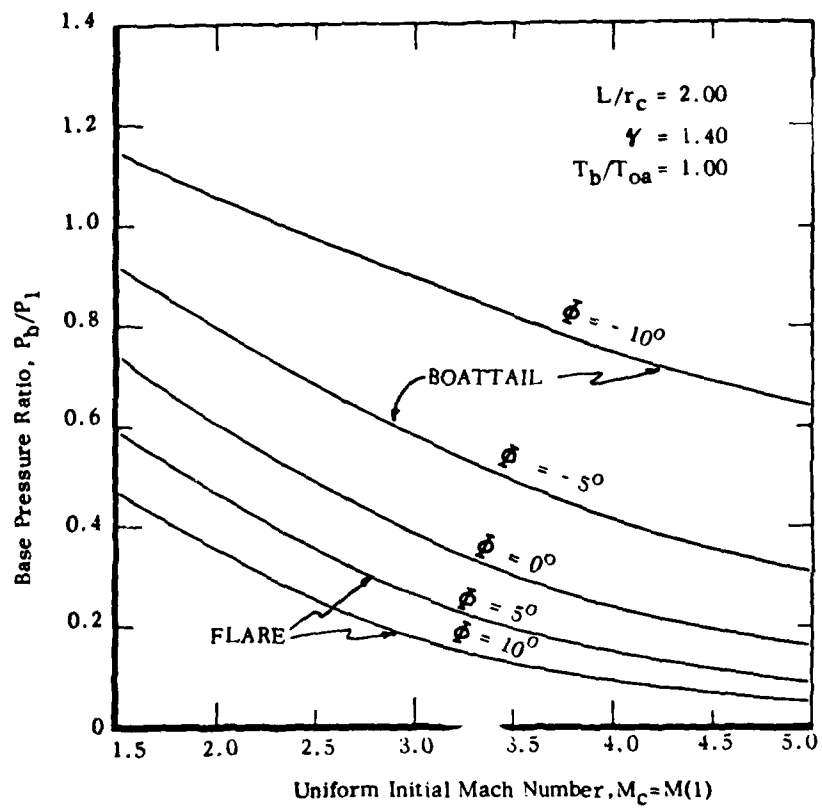


Figure 17. Influence of Initial Mach Number on Base Pressure Ratio for a Fixed Afterbody Length

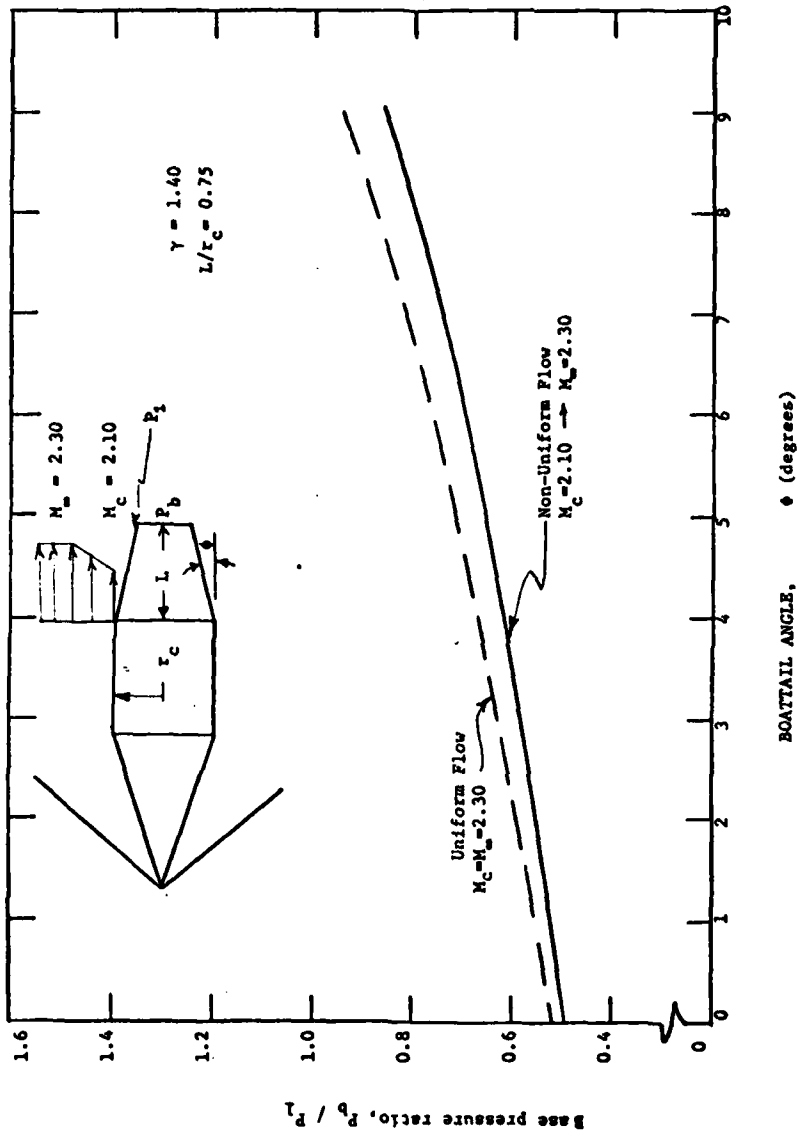


Figure 18. Base Pressure Ratio Versus Boattail Angle for Uniform and Non-Uniform Flow

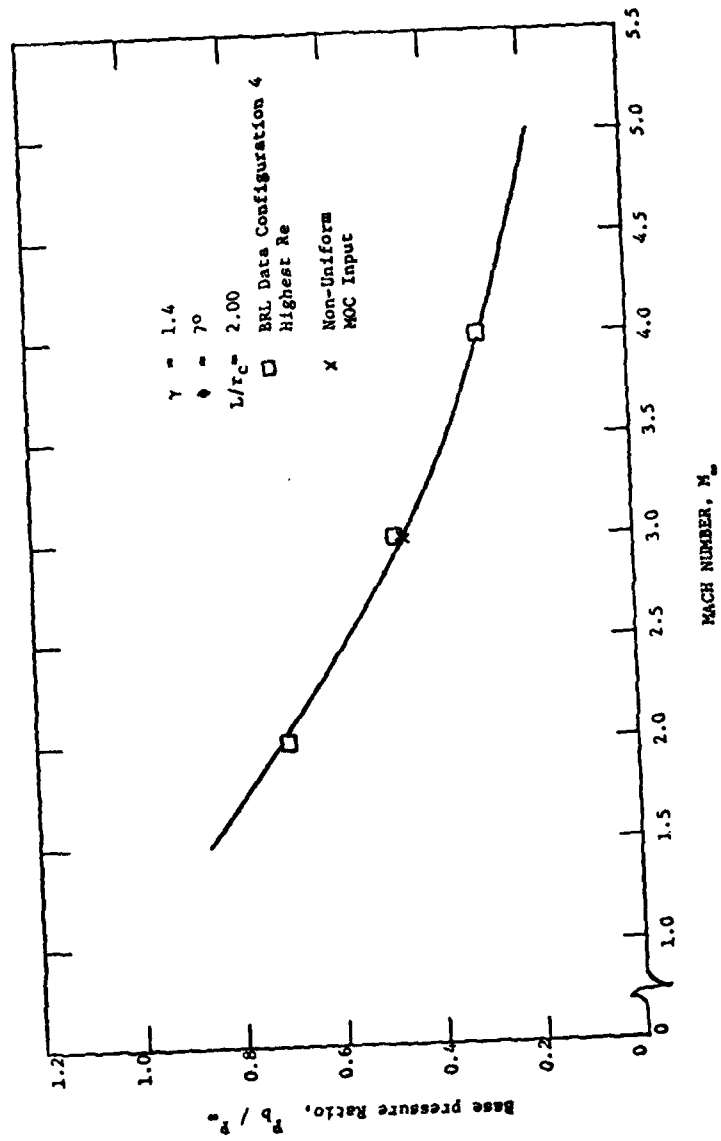


Figure 19. Comparison of the Calculated Base Pressure Ratio for Uniform Flow with BRL Data

REFERENCES

1. Sedney, R., "Review of Base Drag", BRL Report No. 1337, U.S. Army Ballistic Research Laboratory, Aberdeen Proving Ground, Maryland, October 1966. AD 808767
2. Zumwalt, G.W., "Analytical and Experimental Study of the Axially-symmetric Supersonic Base Pressure Problem, Ph.D. Dissertation", University of Illinois, 1959.
3. Mueller, T.J., "Determination of the Turbulent Base Pressure in Supersonic Axisymmetric Flow". *Journal of Spacecraft and Rockets*, Vol. 5, No. 1, pp. 101-107, January 1968.
4. Mueller, T.J., and Hall, C.R., Jr., "Analytical Prediction of the Turbulent Base Pressure in Supersonic Axisymmetric Flow Including the Effect of Initial Flow Direction". AFFDL-TR-68-132, September 1968.
5. Korst, H.H., "A Theory for Base Pressures in Transonic and Supersonic Flow". *Journal of Applied Mechanics*, Vol. 23, No. 4, pp. 593-600, December 1956.
6. Chapman, D.R., "An Analysis of Base Pressure at Supersonic Velocities and Comparison with Experiment". NACA Report 1051, 1951. (Supercedes NACA TN-2137, 1950.)
7. Channapragada, R.S., "Compressible Jet Spread Parameter for Mixing Zone Analyses". *AIAA Journal*, Vol. 1, No. 9, pp. 2188-2189, September 1963.
8. Roache, P.J., and Mueller, T.J., "A FORTRAN IV Program for Calculating the Axisymmetric Base Pressure in Turbulent Supersonic Flow (BASE1)". UNDAS TN-866-M1, University of Notre Dame, Aerospace Engineering, August 1966.
9. Zukoski, E.E., "Turbulent Boundary-Layer Separation in Front of a Forward-Facing Step". *AIAA Journal*, Vol. 5, No. 10, pp. 1746-1753, October 1967.
10. Reid, J., and Hastings, R.C., "Experiments on the Axi-Symmetric Flow Over Afterbodies and Bases at $M = 2.0$ ". Royal Aircraft Establishment Report No. Aero.2628, October 1959, (STAR N66-20065).
11. Sanders, B.R., "Three-Dimensional, Study Inviscid Flow Field Calculations with Application to the Magnus Problem", Ph.D. Dissertation, University of California, Davis, California, May 1974.

LIST OF SYMBOLS

B	Variable defined by Eqn. 2
C	Crocco number
C_p	Pressure coefficient base on M_∞
D	Distance along last characteristic line
D1	Distance along initial characteristic line
I	Subscript
J	Subscript
L	Afterbody length
l	Total body length
M	Mach number
n	Direction perpendicular to streamline
P	Absolute pressure
R	Reference streamline close to but outside of the mixing region; radial location of characteristic grid point; empirical compressible divergence factor
R2	Radial location of grid point along last characteristic
r	Radius
\bar{r}	Radius
s	Direction along a streamline
T	Temperature
u	Velocity in x of X direction
V	Velocity along streamline
X, Y	Coordinates of the reference (inviscid) coordinate system

X	Axial location of grid points in characteristic grid
x, y	Coordinates of the intrinsic (viscous) coordinate system
X2	Axial location of grid point along last characteristic line
α	Dummy variable in Eqn. 14
β	Temperature ratio T_{0a}/T_b
γ	Ratio of specific heats
ξ	Distance along right running wave
η	Distance along left running wave; similarity parameter
θ	Streamline angle
θ_2	Streamline angle at grid point along last characteristic line
μ	Mach angle
ν	Prandtl-Meyer turn angle
ν_2	Prandtl-Meyer turn angle at grid point along last characteristic line
σ	Jet spread parameter
ϕ	Afterbody angle
ϕ	Dimensionless velocity defined as u/u_a

SUBSCRIPTS

1,2,3,4	Refer to conditions at cross-sections of basic flow model
a	Refers to conditions in the external stream adjacent to the mixing region
b	Refers to condition at the base

- c Refers to the conditions upstream of flare or boattail
- d Refers to conditions along a streamline whose kinetic energy is just sufficient to enter the recompression region
- inc Incompressible value
- j Condition along the jet boundary separating streamline
- m Coordinate shift in the mixing theory due to the momentum integral
- o Refers to stagnation conditions
- R Condition along the R streamline
- s Refers to separation conditions
- w Refers to wake
- ∞ Refers to freestream conditions
- () Refers to iteration number

SUPERSCRIPTS

- Average value

BLANK PAGE

APPENDIX A

SYMBOL DEFINITIONS

The symbols used in each subroutine are defined under each subroutine title. The flow model used in the axisymmetric base pressure analysis (Fig. 2) and the afterbody configurations (i.e. boattail or flare shown in Fig. 9) are necessary references for many definitions.

KBPR.CNTROL

BS	=	Afterbody shape
C1	=	$[X2(I)-X2(I-1)]^2$
C2	=	$[R2(I)-R2(I-1)]^2$
CDEL1B	=	Determines distance from body of first point in characteristic field (used at the base)
CDEL1P	=	Determines distance from body of first point in characteristic field (used along the body)
CP	=	Pressure coefficient
D	=	Distance along a characteristic ($= \sqrt{C1 + C2}$)
DEL12	=	XFLARE - XSTART
DEL23	=	XBASE - XFLARE
DINC1	=	Used to calculate maximum spacing of grid points in the characteristic field for the cylindrical surface
DINC2	=	Used to calculate maximum spacing of grid points for afterbody region
DINCB	=	Used to calculate maximum spacing of grid points for the base region
G	=	Ratio of specific heats ($= C_p/C_v$)
G1	=	$-G/(G-1)$
I	=	Subscript
IBOUND	=	Determines type of base pressure solution desired
ILIMA	=	Maximum number of grid points in X-direction
IOPTL	=	Option number permitting variation of input data

IOUT = Determines how characteristics solution will be transferred to base region
 IREAD1 = Determines how initial profile will be set up
 IREAD2 = Determines how characteristics solution will be transferred to the afterbody region
 JLIMA = Maximum number of grid points in R-direction
 JLIMT = Number of points to be read in for a non-uniform profile
 M = Mach number in characteristics field
 MACH = Mach number along initial profile
 MESHPM = Number of discrete turns into which a Prandtl-Meyer expansion is divided
 MIA = Mach number at beginning of characteristics solution at each section
 NU = Prandtl-Meyer turn angle in characteristics field
 NU2 = Prandtl-Meyer turn angle along initial profile
 OMACH = Reference Mach number (usually M_∞)
 PBPINF = P_b/P_∞
 PBPO = P_b/P_0
 PBP1 = P_b/P_1
 PHI = Flare (or boattail) angle (radians)
 PHID = PHI (degrees)
 PINF = P_∞/P_0
 PSURF = P/P_0 along the surface of the body
 PLOPO = P_1/P_0
 R = Radius in characteristic field
 RBASE = Base radius (non-dimensionalized)
 RBODY = Body radius (non-dimensionalized)
 RBODYA = Actual body radius
 RBSRSF = $RBASE/RBODY$ or $XBASE$
 RSRB = R_s/R_{base} where R_s = theoretical sting radius
 R2 = Radius along initial profile
 SMACH = Surface Mach number along body

T = Streamline angle (radians) in characteristics field
 TS = T(1,1)
 T2 = Streamline angle of initial profile
 X = Axial distance in characteristics field
 XBASE = Distance of base from origin
 XFLARE = Distance to the beginning of the afterbody
 XSTART = Distance to the beginning of flow field calculations
 XSURF = Distance along the body surface
 X2 = Axial distance of initial profile

KBPR.FLARE

CANGLE = EMUIA - T(1,1)
 CDEL1 = Determines distance from body of first point in characteristic field
 C1 = $[X2(I) - X2(I-1)]^2$
 C2 = $[R2(I) - R2(I-1)]^2$
 C3AS = $(C3a)^2$
 D = Distance along a characteristic ($= \sqrt{C1 + C2}$)
 DEGNU = Prandtl-Meyer turn angle (degrees)
 DEGT = Streamline angle (degrees)
 DEL = Increment size along initial characteristic
 DELMX = Maximum increment size along initial characteristic
 DEL1 = Size of first increment along initial characteristic
 DINC = Used in the calculation of DELMX
 DTC = TS/NTC
 D1 = Distance along initial profile
 EJK = Used to increment J
 KKJ = Used to increment J
 EMFSRB = Mach number at position 3a in base pressure model
 EMUIA = Mach number at tip of base
 EM2A = Mach number at position 2a in base pressure model
 I = Subscript in axial direction
 IA = Option number used in subroutine KBPR.SETUP

IBOUND = Determines type of base pressure solution desired
 IC = I-1
 ICORN = Number of values of I necessary to turn through an expansion at the surface
 ICRNPT = ICORN + 20
 II = 1/2
 III = Determines body location (= 1 along cylinder part of body; = 2 along afterbody; = 3 in base flow region)
 ILIMA = Maximum number of grid points in X-direction
 J = Subscript in radial direction
 JCORN = Number of values of J necessary to turn through an expansion at the surface
 JLIMA = Maximum number of grid points in R-direction
 JLIMT = Number of points to be read in for a non-uniform profile
 M = Mach number in characteristics field
 MESHPM = Number of discrete turns into which a Prandtl-Meyer expansion is divided
 NTC = Number of turns into which a Prandtl-Meyer expansion is divided
 NTCMIN = Minimum value of NTC
 NU = Prandtl-Meyer turn angle in characteristics field
 NU2 = Prandtl-Meyer turn angle along initial profile
 R = Radius in characteristic field
 RBODYA = Actual body radius
 RLAST = R(L,1)
 RMOD = Dimensionalized radius
 RSRB = R_s/R_{base} where R_s = theoretical sting radius
 R2 = Radius along initial profile
 R2P = R(1,1)
 SINANG = Sin (CANGLE)
 SOL3A = M3A/M2A (or) THET12
 T = Streamline angle (radians) in characteristics field

THET12 = Angle of streamline off base
 THET3A = Angle of streamline at recompression
 TS = T(1,1)
 T2 = Streamline angle of initial profile
 V3A = Prandtl-Meyer turn at R_S (R_S/R_{base} where R_S = theoretical
 sting radius)
 X = Axial distance in characteristics field
 XMOD = Dimensionalized axial distance
 X2 = Axial distance of initial profile
 X2P = X(1,1)

KBPR.LCHAR

C1 = $[X2(I)-X2(I-1)]^2$
 C2 = $[R2(I)-R2(I-1)]^2$
 D = Distance along a characteristic ($= \sqrt{C1 + C2}$)
 DEGNU = Prandtl-Meyer turn angle (degrees)
 DEGT = Streamline angle (degrees)
 EKJ = Used to increment J
 III = Location on body (= 1 along cylindrical part of body;
 = 2 along afterbody; = 3 in base flow region)
 II = Value of I at last point in region 1
 I3 = I + II-1
 JLIMIT = Number of points to be read in for a non-uniform profile
 J1 = I-1
 M = Mach number
 NU = Prandtl-Meyer turn angle in characteristics field
 NU2 = Prandtl-Meyer turn angle along initial profile
 R = Radius in characteristic field
 RATIO = Used to determine closest point to the end of a region
 RBODYA = Actual body radius
 RMOD = Dimensionalized radius
 R2 = Radius along initial profile
 T = Streamline angle (radians) in characteristics field

T2 = Streamline angle of initial profile
X = Axial distance in characteristics field
XMOD = Dimensionalized axial distance
X2 = Axial distance of initial profile

KBPT.SIMR

DX = An increment along the abscissa
I = Subscript
N = Number of increments (even number)
SEV = Sum of the even terms
SOD = Sum of the odd terms
SIMR = Simpsons Rule integration result
X = Value of independent variable
X1 = Lower limit of X
XN = Upper limit of X

KBPT.DINCR

ANG1 = MU-T1
ANG2 = MU-T2
ANG3 = MU-T3
DIFF = JLIMA-23
DINC1 = Used to calculate maximum spacing of grid points in the characteristic field for the cylindrical surface
DINC2 = Used to calculate maximum spacing of grid points for afterbody region
DINCB = Used to calculate maximum spacing of grid points for the base region
H1 = Additional height over regions 2 and 3 which is needed such that a characteristics solution will be complete
H1A = Total height required at XSTART
H1EFF = Effective height at XSTART
H2 = Additional height over region 3 which is needed such that a characteristic solution will be complete

H2A = Total height required at XFLARE
 H2EFF = Effective height at XFLARE
 H3 = Height which is needed such that a characteristics solution will be complete in the base region
 H3A = H3 + RSTING
 H3EFF = Effective height at XBASE
 L1 = XFLARE-XSTART
 L2 = XBASE-XFLARE
 L3 = Length from the base to the sting radius along a 5° angle
 MU = Mach angle
 RBASE = Base radius
 RSTING = Theoretical sting radius
 T1 = A certain percentage of the angle PHI depending on whether PHI is positive or negative (Region 1)
 T12 = Lower limit of flow separation angle from base (= 5°)
 T2 = A certain percentage of the angle PHI depending on whether PHI is positive or negative (Region 2)
 T3 = A certain percentage of the angle PHI depending on whether PHI is positive or negative (Region 3)
 W = Used to convert degrees to radians
 XBASE = Axial distance to base (see Fig. 9)

KBPR.AI1

A = Velocity profile [$= \frac{1}{2} (1 + \operatorname{erf} x)$]
 AI1 = Argument of I1 integral
 CS = (Crocco number)²
 TRB = Base temperature ratio (= T_b/T_{oa})
 TRF = A + TRB (1-A)

KBPR.AI2

A = Velocity profile [$= \frac{1}{2} (1 + \operatorname{erf} x)$]
 AI2 = Argument of I2 integral
 AS = A²

CS = (Crocco number)²
TRB = Base temperature ratio (= T_b/T_{oa})
TRF = A + TRB (1-A)

KBPR.AJ1

A = Velocity profile [$= \frac{1}{2} (1 + \text{erf } x)$]
AJ1 = Argument of J1 integral
CS = (Crocco number)²
TRB = Base temperature ratio (= T_b/T_{oa})
TRF = A + TRB (1-A)

KBPR.AJ2

A = Velocity profile [$= \frac{1}{2} (1 + \text{erf } x)$]
AJ2 = Argument of J2 integral
AS = A²
CS = (Crocco number)²
TRB = Base temperature ratio (= T_b/T_{oa})
TRF = A + TRB (1-A)

KBPR.I1

I1 = Integral I1

KBPR.I2

I2 = Integral I2

KBPR.J1

J1 = Integral J1

KBPR.J2

J2 = Integral J2

KBPR.BODY

DELTA R = $R_{base} - R_{body}$
DELTA X = $X_{base} - X_{flare}$

KBPR.TAB

D1 = Increment of I

DIL = Determines how many points below I will be needed
DIU = Determines how many points above I will be required
I = Subscript
IL = $I - DIL$
IU = $I + DIU$
J = Subscript
P = Lagrange coefficient

KBPR.ERF

A1,A2,A3,A4,A5 = Coefficients
DENOM = Denominator of term
ERF = Error function
X = Point at which erf is to be evaluated
Y = $|x|$

KBPR.PRES

CP = Pressure coefficient
G1 = $-G/G-1$
G2 = $(G-1)/2$
G = Ratio of specific heats
I = Subscript
ILAST = I
ILAST 1 = Value of I at last point on the surface in Region 1
ILAST 2 = Value of I at last point on the surface in Region 2
I1 = I
I2 = $I/2 + 1$
I4,I6 = Dummy integer numbers
M = Mach number
NU = Prandtl-Meyer turn angle
PINFIN = P_0/P_∞
PSURF = P/P_0 along the surface of the body
R = Radius in characteristic field
RE1, RE2, RE3, RE4, RE5, RE6 = Dummy real numbers

RTO = Used to determine last point on surface at each region
SM = Surface Mach number
SMACH = Surface Mach number
T = Streamline angle
X = Axial distance
XSURF = Axial distance of surface

KBPR.RSBF

M1 = Mach number at base
RSBF = Function which describes R_{sting}/R_{base}

KBPR.SIGMA

CS = (Crocco number)²
R = Constant (or) function of CS
SIGMA = Jet spread parameter
SR = Jet spread parameter ratio (= SIGMA/SIGMA_{INCOMP})

KBPR.LINEAR

ACX = Accuracy desired
DX = Increment of X
S = Slope
X1 = Value of X at point 1
X2 = Value of X at point 2
X3 = Projected value of X
XS = Solution of equations
Y1 = Value of Y at point 1
Y2 = Value of Y at point 2
Y3 = Value of Y at point 3

KBPR.CALC

C1 = Inhomogeneous part of characteristic equation at point 1
C13 = Projected value of C from 1 to 3
C2 = Same as C1 except at point 2
C23 = Same as C13 except from 2 to 3
C3 = Final value of inhomogeneous part of equation

ETA23 = Distance along left running wave
 F1 = $Nu1 + T1 + C13 \times Z13$
 F1G = First guess at F1
 F2 = $Nu2 - T2 + C23 \times ETA23$
 F2G = First guess at F2
 MU1 = Mach angle at 1
 MU2 = Mach angle at 2
 MU3G = First guess at Mach angle at 3
 M1 = Mach number at 1
 M2 = Mach number at 2
 M3G = First guess at Mach number at 3
 NU3G = First guess at Prandtl-Meyer turn angle at 3
 R13 = Average radius between 1 and 3
 R23 = Average radius between 2 and 3
 S1 = Slope of right running wave at 1
 S2 = Slope of left running wave at 2
 T3G = First guess at the streamline angle at 3
 Z13 = Distance along right running wave

KBPR.SURF

C1 = (See KBPR.CALC)
 C13 = (See KBPR.CALC)
 DTC = (See KBPR.FLARE)
 I = Subscript
 II = $I/2$
 MU1 = (See KBPR.CALC)
 MU3G = (See KBPR.CALC)
 M1 = (See KBPR.CALC)
 M3G = (See KBPR.CALC)
 NTC = (See KBPR.FLARE)
 NU3G = (See KBPR.CALC)
 R13 = (See KBPR.CALC)
 R2 = Radius at point 2

S1 = (See KBPR.CALC)
S2 = (See KBPR.CALC)
X2 = Axial distance at point 2
Z13 = (See KBPR.CALC)

KBPR.CPB

C13 = (See KBPR.CALC)
IGES = 1
MU1 = (See KBPR.CALC)
MU3G = (See KBPR.CALC)
M1 = (See KBPR.CALC)
M3G = (See KBPR.CALC)
R13 = (See KBPR.CALC)
SMU1 = Sin (MU1)
ST1 = Sin (T1)
S1 = (See KBPR.CALC)
S2 = (See KBPR.CALC)
TP3AV = Average value of the streamline angle at 3
Z13 = (See KBPR.CALC)

KBPR.SEP RTE

MINF = Mach number (free stream)
PRT = Test pressure ratio
PSOPI = P_{sep}/P_{∞}
PSOPIA = P_{sep}/P_{∞}
PSURF = (See KBPR.CNTROL)
PTOPI = P_o/P_{∞}
XSURF = (See KBPR.CNTROL)

KBPR.SETUP

DELINC = New starting position for the characteristic which ends
at the end of a section
D1 = Starting position of characteristic at initial profile
EKJ = Used to increment J

JLIMIT = (See KBPR.CNTROL)
 JST = Subscript
 M = Mach number
 NU = (See KBPR.CNTROL)
 NU2 = (See KBPR.CNTROL)
 R = (See KBPR.CNTROL)
 RTO = Used to determine point closest to end of the region
 R2 = (See KBPR.CNTROL)
 T = (See KBPR.CNTROL)
 T2 = (See KBPR.CNTROL)
 X = (See KBPR.CNTROL)
 X1 = X(I-1,1)
 X2 = (See KBPR.CNTROL)
 X3 = X(I+1,1)

KBPR.PMTURN

ACC = Accuracy desired
 BETA = Defined by equation
 BETA1 = $\sqrt{M_1^2 - 1}$
 BETA2 = $\sqrt{G2}$
 DIFF = BETA1 - BETA2 (used to determine convergence)
 DNU = Function statement
 DNUB = DNU evaluated at BETA2
 G1 = $\sqrt{(G-1)/(G+1)}$
 G2 = 1/G1
 L = Iteration number
 M1 = Mach number upstream
 M2 = Mach number downstream
 NU = Prandtl-Meyer turn angle (function statement)
 NUMAX = Maximum value of Prandtl-Meyer turn angle
 NU1 = NU evaluated at BETA1
 NU2 = NU1 + THETA
 THETA = Isentropic turning angle in degrees

THETAR = Isentropic turning angle in radians

KBPR.PMANGL

A = $\sqrt{(G-1)/(G+1)}$

BETA = $\sqrt{M^2 - 1}$

G = Mach number upstream

PMANGL = Prandtl-Meyer turn angle

KBPR.SOTE2B

AB = Used as a final check for accuracy

AIAC = Defined by equation

CEF = EI/EJ (checks number of solutions)

DX = Increment of X

IAC = AIAC

K = Exponent

L = Determines which root is desired (+1 = upper root;
-1 = lower root)

R1 = XU - XL

SOL1 = Value of function at XU

SOL2 = Value of function at X

T = SOL1 * SOL2

X = Independent variable

XHIGH = Defined by equation

XL = Lower limit of search

XL2 = X

XU = Upper limit of search

XU2 = XHIGH

KBPR.SHOCK

A = Defined by equation

B = - DM*D

C = Defined by equation

D = 1/TD

DD = Detachment turn angle

DM = $\sqrt{M1^2 - 1}$
 G = Ratio of specific heats (= C_p/C_v)
 G1 = $(G-1)/2$
 G2 = $(G+1)/2$
 M1S = $M1^2$
 P = Defined by equation
 PHI = $1/3 \cos^{-1} (\text{PHIARG})$
 PHIARG = Defined by equation
 P3 = Constant
 TD = Tan (DE)
 X = Defined by equation
 Y = Defined by equation

KBPR.FSTEP4

CI2 = Integral I2 evaluated from -3 to +3
 CJ2 = Integral J2 evaluated from -3 to +3
 CR = Ration of Crocco numbers C_{3a}/C_{2a}
 CS = C_{3a}^2
 EGP = Defined by equation (estimated geometric parameter)
 ETAM3D = Three-dimensional value of η_m
 ETAJ = Value of η at separating streamline
 FSTEP4 = EGP - GP
 GP = Geometric parameter
 VI1 = Integral I1 evaluated from η_j to +3
 VJ1 = Integral J1 evaluated from η_j to +3

KBPR.BASE5

ACC5C6 = Accuracy requirement for base pressure solution
 ACST4 = Accuracy requirement for KBPR.SOTE2B subroutine
 C3AS = C_{3a}^2 (C_{3a} = Crocco number at location 3a in base pressure model)
 DXLIN = Increment of X used in KBPR.LINEAR
 G = Ratio of specific heats

IBOUND = (See KBPR.CNTROL)
 IOPT = Printing option number
 M1A = (See KBPR.CNTROL)
 M2A = Mach number at position 2a in base pressure model
 M3AM2A = M3A/M2A
 N = Number of iterations in KBPR.LINEAR
 NASHF = Nash's recompression coefficient
 PBPI = Base pressure ratio, P_b/P_1
 PEST = Estimated base pressure ratio
 PHIJ3 = Velocity ratio along j-streamline
 THETD = THET12 in degrees
 THET12 = (See KBPR.FLARE)
 THET3A = (See KBPR.FLARE)
 THET3D = THET3A in degrees
 TRB = (See KBPR.A11)

KBPR.FBASE5

ACST4 = (See KBPR.FBASE5)
 BS = (See KBPR.CNTROL)
 CI2 = Integral I2 evaluated from -3 to +3
 CJ2 = Integral J2 evaluated from -3 to +3
 CR = Crocco number ratio, $C3A/C2A$
 CS = $C3A^2$
 C1 = Crocco number at 1
 C2A = Crocco number at location 2a in base pressure model
 C2AS = $C2A^2$
 C3A = Crocco number at location 3a
 C3AC2A = $C3A/C2A$
 C3AS = $C3A^2$
 C5 = Defined by equation
 C6 = Defined by equation
 DINC = (See KBPR.CNTROL)
 EGP = (See KBPR.FSTEP4)

ETAJ3 = ETAJ at location 3 (see KBPR.FSTEP4)
 ETAM2D = Value of η_m for two-dimensional flow
 ETAM3D = (See KBPR.FSTEP4)
 FP = (See KBPR.BASE5)
 G = Ratio of specific heats
 GP = Geometric parameter
 G1 = $(G-1)/2$
 G2 = $(G+1)/2$
 G3 = $(G-1)/G$
 G4 = $G/(G-1)$
 IBOUND = (See KBPR.CNTROL)
 IOUT = (See KBPR.CNTROL)
 MESHPM = (See KBPR.CNTROL)
 M1A = (See KBPR.CNTROL)
 M1AS = $M1A^2$
 M2A = (See KBPR.BASE5)
 M2AS = $M2A^2$
 M3AM2A = $M3A/M2A$
 M3A = Mach number at location 3a
 M3AS = $M3A^2$
 PHI = Velocity ratio
 PHIJ3 = Velocity ratio along j-streamline
 PNASH = Pressure with Nash's recompression coefficient
 P1P3 = P_1/P_3
 P2P3 = P_2/P_3
 P4P3 = P_4/P_3
 ROBDY = (See KBPR.CNTROL)
 RBSRSF = (See KBPR.CNTROL)
 RSRB = (See KBPR.FLARE)
 THET12 = (See KBPR.FLARE)
 THET3A = (See KBPR.FLARE)
 TR = $1./TRB$ (see KBPR.A11)

TRB = (See KBPR.AI1)
XBASE = (See KBPR.CNTROL)

KBPR.SEP RTE

MINF = Mach number (free stream)
PRT = Test pressure ratio
PSOPI = P_{sep}/P_{∞}
PSOPIA = P_{sep}/P_{∞} at the free stream Mach number
PSURF = (See KBPR.CNTROL)
PTOPI = P_o/P_{∞}
XSURF = (See KBPR.CNTROL)

APPENDIX B

OPERATING INSTRUCTIONS

To operate this computer program, a minimum of eleven cards must be read in. The maximum number of cards is a function of the type of Mach number profile desired as input.

1) READ BS, XSTART, XFLARE, PHI, RBSRSF, RBODYA, IOPTL

BS is the shape of the afterbody which is desired. This program has a capability to analyze only a conical flare or boattail. This corresponds to $BS = 1$. Any other read-in will result in a termination of the program. It should be noted that the term BS has been declared to be an integer number.

XSTART is the X-coordinate which locates the beginning of the characteristics solution over the body. This XSTART position falls on the cylindrical part of the body of revolution. XSTART need not be zero. XSTART is read in the machine as a real number. (See Fig. 9)

XFLARE is the X-coordinate which locates the beginning of the afterbody. ($XFLARE \geq XSTART$). This again is a real number. For $XFLARE = XSTART$, no characteristics solution is done over the cylindrical portion of the body, but instead, the characteristics begin immediately before the afterbody region. (See Fig. 9)

PHI is the angle of the flare or boattail in degrees. This is

a real number once again. For a flare, PHI is a positive number, while for a boattail, PHI is negative. (See Fig. 9)

RBSRSF may mean one of two things depending on the type of input desired. This real number may mean: (See Fig. 9)

a) $R_{\text{base}}/R_{\text{body}}$ where R_{base} is the radius of the base and R_{body} is the radius of the cylindrical portion of the body. This particular input is achieved by setting IOPTL = 1.

b) X_{base} which is the X-coordinate of the base of the body. This corresponds to IOPTL = 2.

RBODYA is the radius of the body. This real number may be read in as any unit of length desired (i.e., feet, calibers, etc.), but it is necessary that the units on the X-dimensions be the same as that of RBODYA.

IOPTL is an integer option number which permits a variation in input. (See RBSRSF explanation).

SAMPLE CARDS:

(A) 1,0.00, 1.00, - 10.0, 0.60, 1.00, 1

This corresponds to a body with a 10° boattail whose $R_{\text{base}}/R_{\text{body}} = 0.60$. In addition, a characteristics solution is performed along the cylindrical portion of the body for an X-distance of 1.0.

(B) 1,0.00, 0.00, 0.00, 0.00, 1.00, 2

This particular input would result in just a base pressure solution.

(C) 1,1.00, 1.00, 5.00, 2.00, 1.00, 2

This corresponds to a body with a 5° flare whose afterbody length is 2.0 radii.

2) READ G, M(1), OMACH

G is the ratio of specific heats ($= C_p/C_v$). This is a real number. For air, $G = 1.40$.

M(1) is the surface Mach number at the point at which the characteristics solution begins.

OMACH is the free stream Mach number. Actually this may be any reference Mach number and, for example, may refer to the Mach number ahead of the shock for a projectile.

SAMPLE CARD:

1.40, 2.50, 3.00

3) READ IREAD1, IREAD2, IOUT

IREAD1 determines how the initial Mach number profile is to be set up for analysis. IREAD1, an integer number, corresponds to the position, XSTART.

IREAD2 determines how the profile will be transferred from the cylindrical body to the afterbody. This corresponds to the position XFLARE.

IOUT determines how the profile will be transferred from the afterbody region to the base region. This corresponds to the position XBASE.

General Comments on IREAD1, IREAD2, IOUT

These are all integer numbers which are defined for 0, 1, 2.

If IREAD1 = 0, then a uniform profile is assumed at XSTART. If IREAD1 = 1, then a profile along a line perpendicular to the body is read in. If IREAD1 = 2, then a profile is read in which is along a characteristic.

It must be noted that if XFLARE = XSTART, then IREAD1 = IREAD2. Similarly, if XSTART = XFLARE = XBASE, then IREAD1 = IREAD2 = IOUT.

SAMPLE CARDS:

(A) 0, 1, 2

Uniform profile at XSTART; transfer from the cylindrical body to the afterbody along a line which is nearly perpendicular to the body; transfer to base region along a characteristic line.

(B) 0, 0, 0,

This card would represent a base pressure solution with a uniform profile read-in.

CAUTION: Only an irrotational profile may be read into the program. A rotational Mach number profile (e.g., a viscous profile) cannot be used correctly since the characteristics solution requires an irrotational flow.

4) READ MESHPM, CDEL1B, CDEL1P

MESHPM is an integer number which determines the number of individual discrete turns into which the boattail angle is divided. Usually, MESHPM = 2 is sufficient. This is also used in the base pressure solution for the same reason.

CDEL1B is a real number which sets the increment of the first point off the surface along a characteristic. CDEL1B is used in the base region.

CDEL1P is again a real number which sets the increment of the first point off the surface along a characteristic on the body.

General Comments:

CDEL1B = 0.01 and CDEL1P = 0.10 is sufficient for good accuracy.

5) READ JLIMIT

JLIMIT is the number of cards which will be read into the program which describes the initial Mach number profile. This card is not read if IREAD1 = 0.

6) READ X2(I), R2 (I), MACH, T2 (I)

X2 (I) is the X-coordinate of various points in the initial profile.

R2 (I) is the R-coordinate of various points in the initial profile.

MACH is the Mach number at the point X(I), R(I).

T2 (I) is the streamline angle (in degrees) at the point X(I), R(I).

General Comments

There must be a total of JLIMIT cards read into the program with each card containing the above quantities for a single point. The first card must describe conditions on the surface and subsequent cards proceed outward from the body.

There must be at least two cards read into the program, and the maximum number of cards is 60.

- 7) READ 31
- 8) READ 32
- 9) READ 33

These three read statements are run identification statements. These may be punched with alpha-numeric characters not exceeding 55 spaces. These three data cards will be printed at the beginning of the base pressure section.

- 10) READ DXLIN, ACST4, ACC5C6, NASHF, IOPT

DXLIN is a real number which is used in the LINEAR subroutine. A function is evaluated at some value X and once again at the value X-DXLIN. A typical value for DXLIN is 0.005. However, larger values may be used if so desired.

ACST4 is an accuracy requirement which is used in the SOTE2B subroutine. This determines to what accuracy a function is to be solved. A reasonable value of ACST4 is 0.005.

ACCSC6 is an accuracy requirement used in determining the base pressure ratio, P_b/P_1 . A typical value for ACCSC6 is 0.001.

NASHF is Nash's recompression coefficient which has been assumed to be 1.0.

IOPT is a printing option number. If IOPT = 2 then the base pressure parameters are printed out. If IOPT \neq 2, then printing is suppressed.

11) READ IBOUND

IBOUND is an integer number which determines which type of base pressure solution is desired. IBOUND = 1 for a conetail solution or IBOUND = 2 for a constant pressure solution.

12) READ PEST, TRB

PEST is the estimated base pressure ratio, P_b/P_1 . For most reasonable guesses at the base pressure at moderate flare or boattail angles, the program does converge. However, for large angles, coupled with a poor guess, the program may terminate. It is recommended that a guess be made which is close to the assumed answer, since the calculation procedure is relatively lengthy.

TRB is the temperature ratio, T_b/T_{oa} , where T_b is the base temperature and T_{oa} is the free stream stagnation temperature.

General Notes:

This read statement is also used as a control statement. If PEST < 0, the program starts over and a new case is run.

However, if $TRB < 0$, then a new base pressure solution may be obtained in which the temperature ratio may be varied. This, of course, implies that the flow along the body remains the same.

For example if just one case is to be run, the last two cards will be:

0.820, 1.00

-1.0, 1.0

However, if two temperature ratios are desired, then an additional card is used:

0.820, 1.00

0.900, 0.80

-1.0, 1.0

APPENDIX C
BOATTAIL/FLARE-BASES
COMPUTER PROGRAM INPUT AND OUTPUT
FOR THE ABERDEEN PROVING
GROUND UNIVAC 1108
(SAMPLE CASES INCLUDED).

SAMPLE INPUT-OUTPUT FOR
UNIFORM APPROACH FLOW ($M_c = 3.0$)
 AND A ONE CALIBER 7° CONICAL
 BOATTAIL WITH $\gamma = 1.4$ AND $T_b/T_{oa} = 1.0$.

```

WTB*KBPR(1).BPD
1 1,0.00,0.00,-7.00,2.000,1.000,2
2 1.40,5.00,5.00
3 0,0,1
4 2,0.01,0.10
5 SOC BOATTAIL BASE PRESSURE
6 M=3.00, PHI=-7.00 DEG
7 6 CAL MODEL. 1 CAL BOATTAIL
8 0.005,0.005,0.001,1.0,2
9 1
10 0.65,1.00
11 -1.0,1.0
  
```

```

#MAP.S
MAP28R1 PL71-3 08/25/77 14:13:55
1. IN KBPR.MAIN
2. IN KBPR.FLARE
3. IN KBPR.LCHAR
4. IN KBPR.SIMR
5. IN KBPR.DINCR
6. IN KBPR.AI1L
7. IN KBPR.AI2L
8. IN KBPR.AJ1L
9. IN KBPR.AJ2L
10. IN KBPR.I1
11. IN KBPR.I2
12. IN KBPR.J1
13. IN KBPR.J2
14. IN KBPR.BODY
15. IN KBPR.TAB
16. IN KBPR.ERF
17. IN KBPR.PRES
18. IN KBPR.RSBF
19. IN KBPR.SIGMA
20. IN KBPR.LINEAR
21. IN KBPR.CALC
22. IN KBPR.SURF
23. IN KBPR.CPB
24. IN KBPR.SEPRTE
25. IN KBPR.SETUP
26. IN KBPR.PMTURN
27. IN KBPR.PMANGL
28. IN KBPR.SOTE2B
29. IN KBPR.SHOCK
30. IN KBPR.FSTEP4
31. IN KBPR.BASE5
32. IN KBPR.FBASE5
  
```

M(INFINITY) = 3.00

P(INFINITY)/PT = .0272

PHI = -7.00 DEGREES

UNIFORM PROFILE WITH M = 3.000

X	M	P/PT	CP
.000	3.000	.0272	.0000
.001	3.188	.0206	-.0387
.001	3.391	.0153	-.0694
.001	3.391	.0153	-.0694
.005	3.391	.0153	-.0694
.109	3.387	.0154	-.0689
.162	3.383	.0155	-.0684
.216	3.379	.0156	-.0678
.270	3.375	.0157	-.0673
.323	3.371	.0158	-.0668
.377	3.367	.0159	-.0663
.430	3.363	.0159	-.0658
.484	3.359	.0160	-.0652
.538	3.356	.0161	-.0647
.591	3.352	.0162	-.0642
.645	3.348	.0163	-.0637
.699	3.344	.0164	-.0631
.752	3.340	.0165	-.0626
.806	3.336	.0166	-.0621
.859	3.333	.0167	-.0615
.913	3.329	.0168	-.0610
.967	3.325	.0169	-.0605
1.020	3.321	.0169	-.0599
1.074	3.317	.0170	-.0594
1.193	3.314	.0171	-.0588
1.312	3.305	.0173	-.0576
1.432	3.297	.0176	-.0564
1.551	3.289	.0178	-.0552
1.670	3.281	.0180	-.0539
1.790	3.272	.0182	-.0527
1.909	3.264	.0184	-.0514
2.000	3.256	.0186	-.0501
2.000	3.250	.0189	-.0491

TRUNID = 1 DJNC = .0659 CHELL = .0100 MESIPM = 2 10PT = 2
DXLIN = .00500 G = 1.400 ACST4 = .00500 ACCUSC6 = .00100 NASHF = 1.000

CONETAIL SOLUTION

.65000
.64500
.70193
.68263

M/A = 3.2499 G = 1.400 TB/TOA = 1.000 PB/P1 = .6826 N = 2 THEID = 11.415
ETAJ3 = .1216 PHJ3 = .5683 ETAM3D = .8865 ETAM2D = 1.0801
GP = .3295+02 ECP = .3115+02 MZA = 3.5151 MSA/MZA = .8935 CJA**2 = .6636
THEI3D = 11.4155

PB/P(INF) = .4714 PB/PO = .0128

SAMPLE INPUT-OUTPUT FOR THE
NON-UNIFORM APPROACH FLOW
 OBTAINED FROM BRL METHOD OF
 CHARACTERISTICS PROGRAM AND
 A ONE CALIBER 7° CONICAL BOATTAIL
 WITH $\gamma = 1.4$ AND $T_b/T_{oa} = 1.0$.

```

WTR*KBPR(1).BPDAT
 1  1.000,0.000,-7.00,2.000,1.00,2
 2  1.40,3.135,3.00
 3  1,1,2
 4  2,0.01,0.10
 5  22
 6  0.000,1.000,3.050,0.000
 7  0.000,1.000,3.050,0.000
 8  0.000,1.200,3.050,0.000
 9  0.000,1.300,3.070,0.000
10  0.000,1.400,3.100,0.000
11  0.000,1.500,3.080,0.000
12  0.000,1.600,3.050,0.000
13  0.000,1.700,3.000,0.000
14  0.000,1.800,2.960,0.000
15  0.000,1.900,2.920,0.000
16  0.000,2.000,2.890,0.000
17  0.000,2.100,2.860,0.000
18  0.000,2.200,2.850,0.000
19  0.000,2.300,2.830,0.000
20  0.000,2.400,2.820,0.000
21  0.000,2.500,2.860,0.000
22  0.000,2.600,2.970,0.000
23  0.000,2.700,3.000,0.000
24  0.000,2.800,3.000,0.000
25  0.000,2.900,3.000,0.000
26  0.000,3.000,3.000,0.000
27  0.000,3.100,3.000,0.000
28  SOC-BOATTAIL BASE PRESSURE
29  M=3.00, PHI=-7.00 DEG
30  6 CAL MODEL - 1 CAL BOATTAIL
31  0.005,0.005,0.001,1.0,2
32  1
33  0.750,1.00
34  -1.0,1.0
  
```

MAP,S
MAP28R1 RL71-3 08/25/77 14:59:50

1. IN KBPR.MAIN
2. IN KBPR.FLARE
3. IN KBPR.LCHAR
4. IN KBPR.SIMR
5. IN KBPR.DINCR
6. IN KBPR.AI1L
7. IN KBPR.AI2L
8. IN KBPR.AJ1L
9. IN KBPR.AJ2L
10. IN KBPR.I1
11. IN KBPR.I2
12. IN KBPR.J1
13. IN KBPR.J2
14. IN KBPR.BODY
15. IN KBPR.TAB
16. IN KBPR.ERF
17. IN KBPR.PRES
18. IN KBPR.RS8F
19. IN KBPR.SIGMA
20. IN KBPR.LINEAR
21. IN KBPR.CALC
22. IN KBPR.SURF
23. IN KBPR.CPB
24. IN KBPR.SEP RTE
25. IN KBPR.SETUP
26. IN KBPR.PMTURN
27. IN KBPR.PMANGL
28. IN KBPR.SOTE2B
29. IN KBPR.SHOCK
30. IN KBPR.FSTEP4
31. IN KBPR.BASE5
32. IN KBPR.FBASES

M(INFINITY) = 3.000

P(INFINITY)/PT = .0272

PHI = -7.00 DEGREES

NON-UNIFORM PROFILE

X	M	P/PT	CP
.000	3.050	.0253	-.0114
.001	3.242	.0190	-.0478
.001	3.449	.0141	-.0765
.001	3.449	.0141	-.0765
.056	3.449	.0141	-.0765
.111	3.445	.0142	-.0761
.166	3.441	.0143	-.0756
.221	3.437	.0143	-.0751
.276	3.433	.0144	-.0746
.331	3.429	.0145	-.0741
.385	3.425	.0146	-.0736
.440	3.421	.0147	-.0731
.495	3.417	.0148	-.0726
.550	3.413	.0149	-.0721
.605	3.409	.0149	-.0717
.660	3.405	.0150	-.0712
.715	3.401	.0151	-.0707
.771	3.397	.0152	-.0702
.828	3.396	.0152	-.0700
.885	3.395	.0152	-.0699
.943	3.395	.0152	-.0699
1.001	3.395	.0152	-.0699
1.059	3.395	.0152	-.0699
1.117	3.394	.0152	-.0698
1.237	3.394	.0152	-.0698
1.358	3.398	.0152	-.0702
1.481	3.401	.0151	-.0707
1.591	3.405	.0150	-.0711
1.693	3.396	.0152	-.0700
1.794	3.380	.0156	-.0680
1.892	3.365	.0159	-.0659
1.985	3.348	.0163	-.0637
2.000	3.329	.0168	-.0610

IN FLARE AT MAX I = 118 N = .561.GT.NSRB = .441. T = -.1800, N = .8436

MIA = 3.5256 G = 1.400 TB/TDA = 1.000 PB/PI = .7483 N = 1 TIME/D = 10.313
ETAJ3 = .0806 PHIJ3 = .5454 ETAM3D = .7390 ETAM2D = 1.2949
GP = .2352*02 EGP = .2292*02 M2A = 3.5280 M3A/M2A = .8026 C3A**2 = .6159
TIME3D = 10.3128

PR/P(JNF) = .4628 PB/PO = .0126

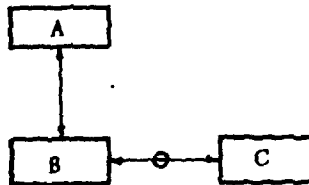
APPENDIX D
COMPUTER PROGRAM
FLOW CHARTS

NOTATION:

1. Main Program or subprogram 
2. "COMMON" block  ; information is transferred between subprograms F1 and F2 through COMMON block C1.

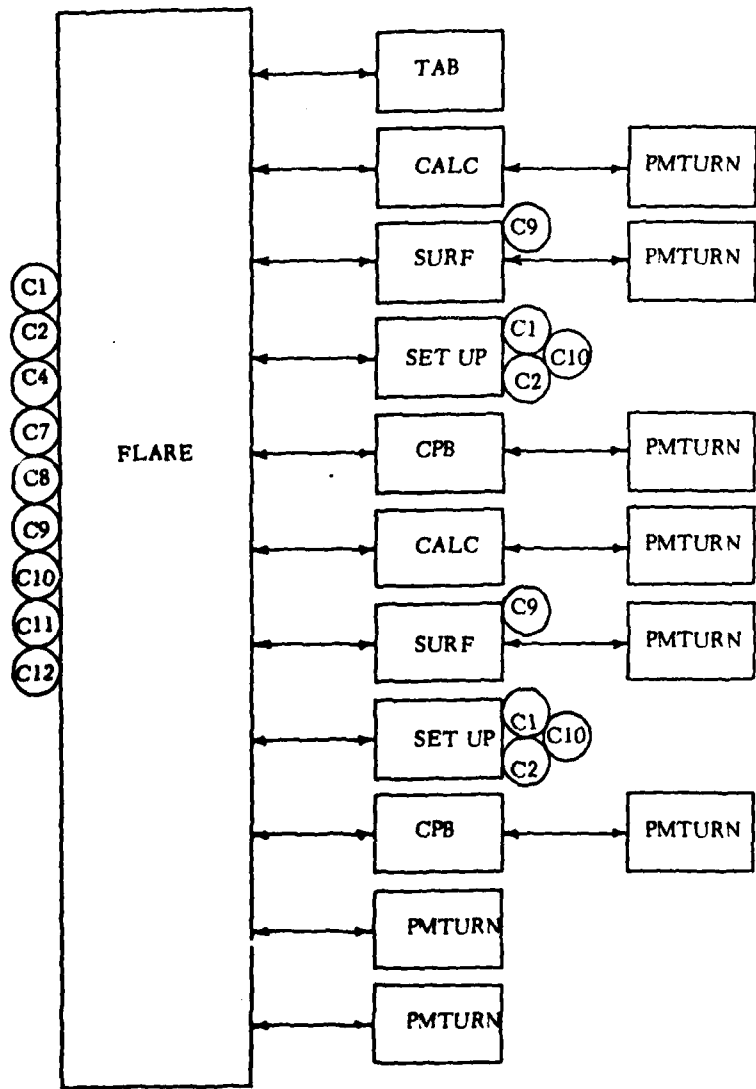


3. Subprogram CALL's

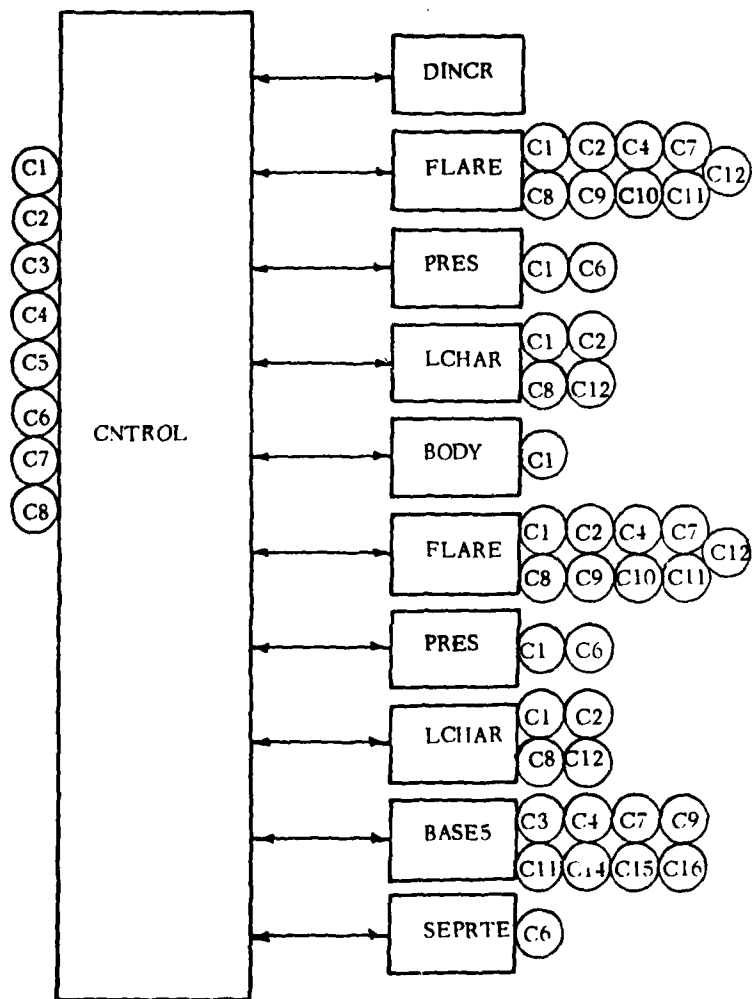


B CALL's C as explicitly instructed in A.
That is, C is an EXTERNAL function to A's
CALL to B.

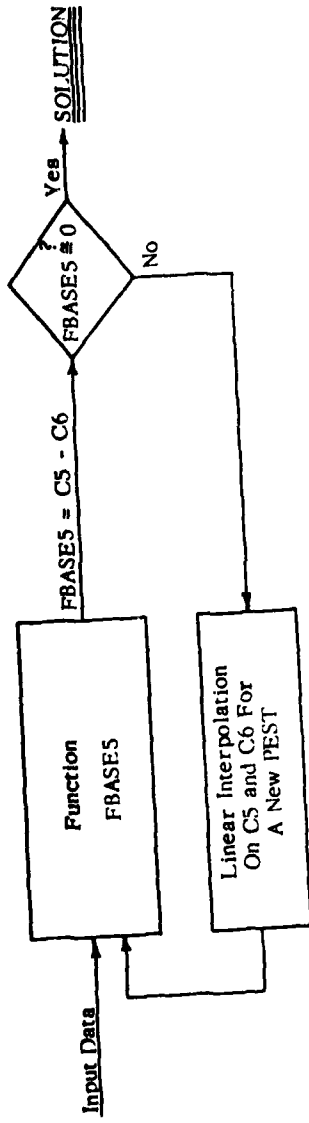
The order of execution generally proceeds from top to bottom and/or from left to right. Internal functions such as SQRT, TAN, etc. are not shown.



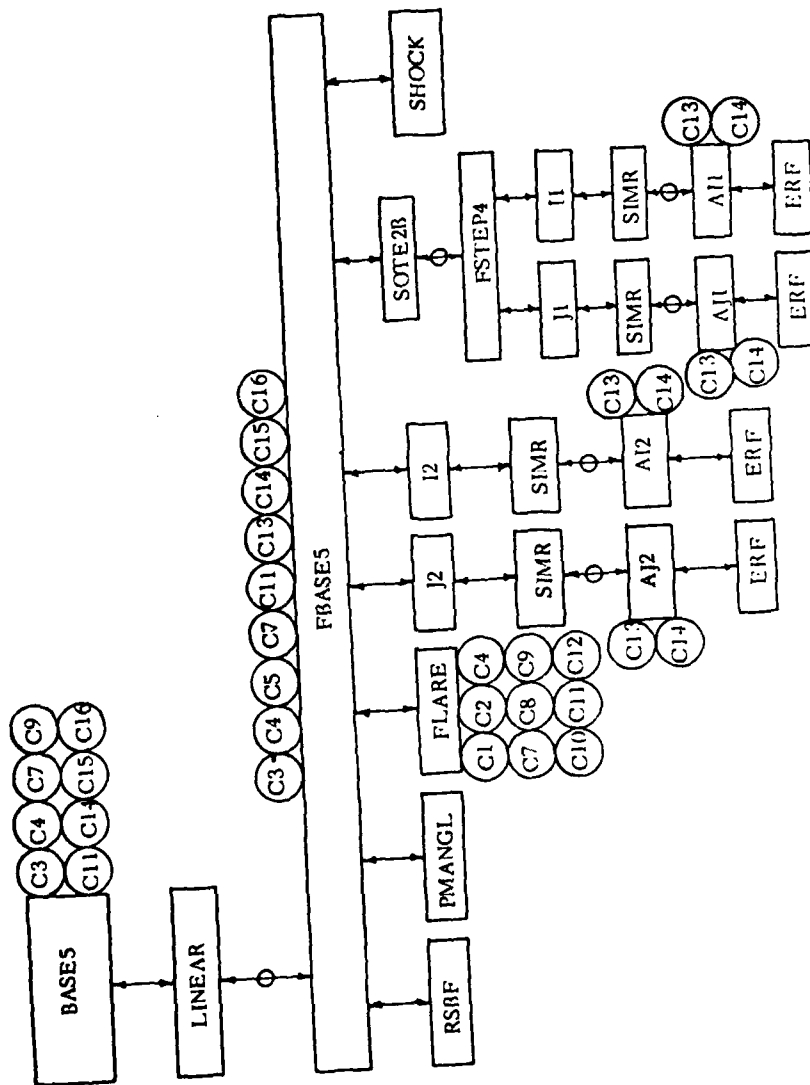
Flow Chart 1



Flow Chart 2



Flow Chart 3



Flow Chart 4

DISTRIBUTION LIST

<u>No. of Copies</u>	<u>Organization</u>	<u>No. of Copies</u>	<u>Organization</u>
12	Commander Defense Technical Info Center ATTN: DDC-DDA Cameron Station Alexandria, VA 22314	1	Director US Army Air Mobility Research and Development Laboratory Ames Research Center Moffett Field, CA 94035
1	Commander US Army Materiel Development and Readiness Command ATTN: DRCDMD-ST 5001 Eisenhower Avenue Alexandria, VA 22333	1	Commander US Army Communications Research and Development Command ATTN: DRDCO-PPA-SA Fort Monmouth, NJ 07703
9	Commander US Army Armament Research and Development Command ATTN: DRDAR-TSS (2 cys) DRDAR-LCA-F Mr. D. Mertz Mr. E. Falkowski Mr. A. Loeb Mr. R. Kline Mr. S. Kahn Mr. S. Wasserman Mr. H. Hudgins Dover, NJ 07801	1	Commander US Army Electronics Research and Development Command Technical Support Activity ATTN: DELSD-L Fort Monmouth, NJ 07703
1	Commander US Army Armament Materiel Readiness Command ATTN: DRSAR-LEP-L, Tech Lib Rock Island, IL 61299	2	Commander US Army Missile Command ATTN: DRSMI-R DRSMI-RDK Mr. R. Deep Redstone Arsenal, AL 35809
1	Director US Army Armament Research and Development Command ATTN: DRDAR-LCB-TL Watervliet, NY 12189	1	Commander US Army Missile Command ATTN: DRSMI-YDL Redstone Arsenal, AL 35809
1	Commander US Army Aviation Research and Development Command ATTN: DRDAV-E 4300 Goodfellow Blvd. St. Louis, MO 63120	1	Commander US Army Tank Automotive Research and Development Command ATTN: DRDTA-UL Warren, MI 48090
		1	Director US Army TRADOC Systems Analysis Activity ATTN: ATAA-SL, Tech Lib White Sands Missile Range, NM 88002

DISTRIBUTION LIST

<u>No. of Copies</u>	<u>Organization</u>	<u>No. of Copies</u>	<u>Organization</u>
1	Commander US Army Research Office P. O. Box 12211 Research Triangle Park NC 27709	1	Director NASA Ames Research Center ATTN: MS-227-8 Dr. L. Schiff Moffett Field, CA 94035
1	Commander US Naval Air Systems Command ATTN: AIR-604 Washington, D. C. 20360	3	Sandia Laboratories ATTN: Technical Staff, Dr. W.L. Oberkamp Aeroballistics Division 5631, G.R. Eisner H.R. Vaughn Albuquerque, NJ 87184
2	Commander David W. Taylor Naval Ship Research and Development Center ATTN: Dr. S. de los Santos Mr. Stanley Gottlieb Bethesda, Maryland 20084	1	Massachusetts Institute of Technology ATTN: Tech Library 77 Massachusetts Avenue Cambridge, MA 02139
4	Commander US Naval Surface Weapons Center ATTN: Dr. T. Clare, Code DK20 Mr. P. Daniels Mr. D. A. Jones III Mr. L. Mason Dahlgren, VA 22448	1	Stanford University Department of Aeronautics and Astronautics ATTN: Prof. J. Steger Stanford, CA 94035
3	Commander US Naval Surface Weapons Center ATTN: Code 312 Dr. C. Shieh Dr. W. Yanta Mr. R. Voisint Silver Spring, MD 20910	1	University of California, Davis Department of Mechanical Engineering ATTN: Prof. H.A. Dwyer Davis, CA 95616
1	Commander US Naval Weapons Center ATTN: Code 3431, Tech Lib China Lake, CA 93555	1	University of Colorado Department of Aerospace Engineering ATTN: Prof. G. Inger Boulder, CO 80309
1	Director NASA Langley Research Center ATTN: NS-185, Tech Lib Langley Station Hampton, VA 23365		

DISTRIBUTION LIST

<u>No. of Copies</u>	<u>Organization</u>
1	University of Colorado Department of Aerospace Engineering ATTN: Prof. G. Inger Boulder, CO 80309
1	University of Delaware Mechanical and Aerospace Engineering Department ATTN: Dr. J. E. Danberg Newark, DE 19711
1	University of Florida ATTN: Dr. J.E. Milton P.O. Box 1918 Eglin AFB, FL 32542
1	University of Notre Dame Department of Aeronautical and Mechanical Engineering ATTN: Prof. T. J. Mueller Notre Dame, IN 46556

Aberdeen Proving Ground

Dir, USAMSAA
ATTN: DRXSY-D
DRXSY-MP, H. Cohen

Cdr, USATECOM
ATTN: DRSTE-TO-F

Dir, USACSL, Bldg. E3516, EA
ATTN: DRDAR-CLB-PA

END